



MADYN 2000 Version 4.0

The following new features and improvements were introduced in version 4.0:

1. [Reorganisation of Connections](#)
2. [New Gear Connection Facilitating Double Meshes and Inner Meshes \(for planetary gears\)](#)
3. [New Connection Facilitating Rotating Planets of Planetary Gears](#)
4. [New Shaft Connections Facilitating the Modelling of Shaft in Shaft Designs](#)
5. [New Nonlinear Capabilities](#)
6. [Active Systems \(apart from radial magnetic bearings\)](#)
7. [Rolling Element Bearings](#)
8. [Squeeze Film Damper](#)
9. [Improvements and New Features for Fluid Film Bearings](#)
10. [New Features for Static Analyses](#)
11. [Extension of Modelling Objects](#)
12. [Improved Loading of Fluids](#)
13. [Improvements in Plots](#)
14. [Improvements in Prints](#)

Table of content for detailed description of features:

1. Reorganisation of Connections.....	2
1.1 Rigid Connection	3
1.2 Connection via Flexible Coupling	4
2. New Gear Connection Facilitating Double Meshes and Inner Meshes.....	5
3. New Connection Facilitating Rotating Planets of Planetary Gears	7
4. New Shaft in Shaft Connection via Radial Bearings	9
5. New Nonlinear Capabilities.....	11
5.1 Flexible Coupling Nonlinearities: Rubber Coupling and Slipping Coupling	11
5.2 General Nonlinearities	17
6. Active Systems (apart from magnetic bearings)	21
6.1 Axial Magnetic Bearing	21
6.2 Active Torsional System	24
6.3 Imported Transfer Function in Table Form	27
7. Rolling Element Bearings	28
8. Squeeze Film Damper (SFD)	34
8.1 Squeeze Film Damper in a Floating Ring Bearing	34
8.2 General Squeeze Film Damper (Standard Bearing)	36
9. Improvements and New Features for Fluid Film Bearings	36
9.1 General Improvements	36
9.2 Closed Cylindrical Bearing.....	36
10. New Features for Static Analyses.....	39
10.1 Alignment Sensitivity Analysis	39
10.2 Speed Dependent Loads	41
11. Extension of Modelling Objects	43
11.1 General Spring (with off diagonal elements).....	43
11.2 Flexible Coupling Damping.....	45
12. Improved Loading of Fluids	45
13. Improvements in Plots	46
13.1 Plot Editing	46
13.2 Model Plots.....	46
13.2 Shape Plots (data cursor).....	49
14. Improvements in Prints.....	50
14.1 System Print	50
14.2 Print of Radial Fluid Film Bearings	51
References	53



1. Reorganisation of Connections

In MADYN 2000 there are several connectors to connect shafts:

- The simple rigid connection directly connecting two shafts.
- Flexible couplings connect shafts via coupling properties.
- Gears connect several shafts via gear mesh properties.

In version 4.0 there is the following new connection with the purpose to connect an inner and outer shaft via any radial bearing:

- Shaft-in-Shaft Connection.

In case of the shaft in shaft connection, the inner shaft requires a spring bearing support SBS. The bearing is mounted between the inner shaft and the SBS. The outer shaft then is connected to the SBS with a rigid connection for the radial displacements. For this connection the SBS functions as connector.

In version 4.0 the different connections can be created in the following GUIs:

- System GUI (as in previous versions)
- In the connector GUI, i.e. in the SBS GUI (spring bearing support), the FCP GUI (flexible coupling) and the GER GUI (gear)
- In the station GUI

The system GUI can be seen in figure 1.1. Its appearance has slightly changed. It gives an overview of all connections in a system. Clicking on the button “Connections” opens a GUI to edit connections.

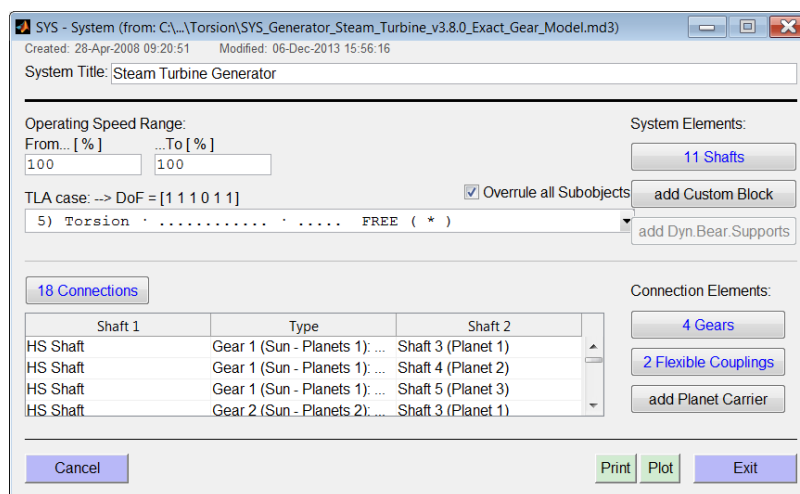


Fig. 1.1: System GUI with overview of connections

The options to create connections from the connector GUI and station GUI are new. The actual connection GUI for all possible connections is more or less the same. Several of its variants are shown in the following chapters.

The gear connection with new features is explained in detail in chapter 2, the new shaft in shaft connection in chapter 3 and the planet carrier connection in chapter 4.

The additional options for the rigid connection and the FCP are explained in the following two sub-chapters 1.1 and 1.2.



1.1 Rigid Connection

The station GUI with the new button “add Rigid Connection” can be seen in figure 1.2. The new button opens the connection GUI shown in figure 1.3

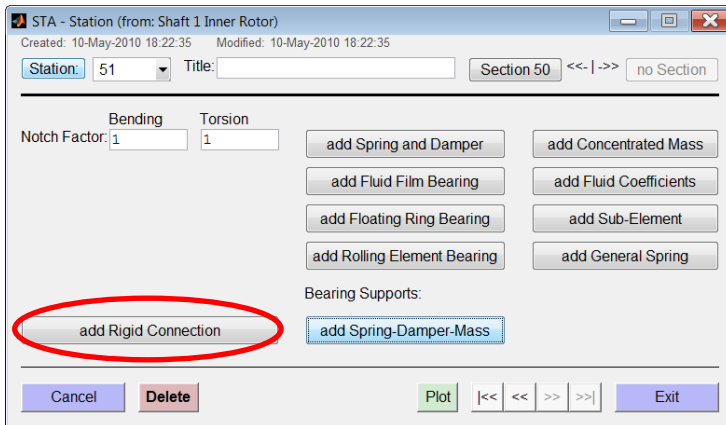


Fig. 1.2: Station GUI

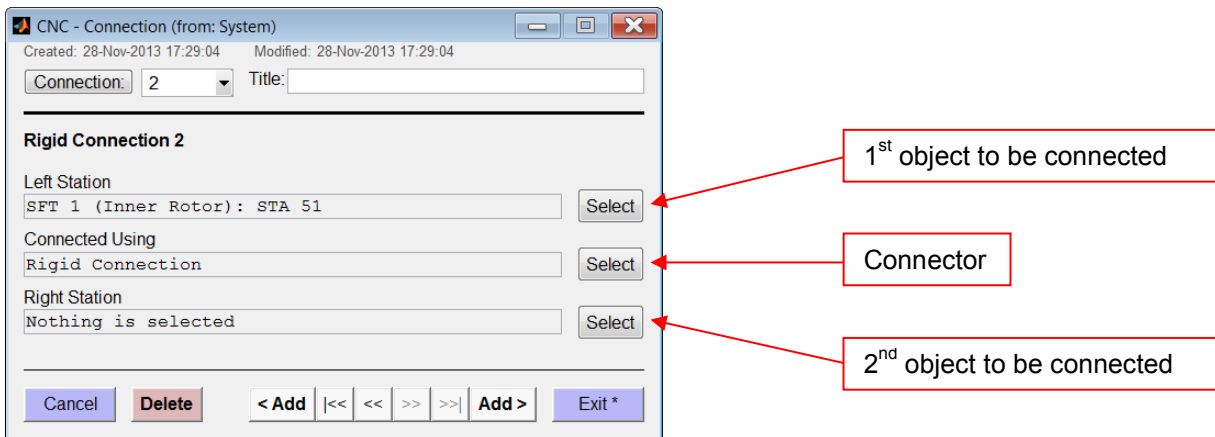


Fig.1.3: Connection GUI called from Station

The connection GUI has three fields with the connector in the middle and the objects to be connected in the top and bottom fields. As default the shaft and station from which the connection GUI has been opened is shown in the top field as first object and a “Rigid Connection” as connector. The second object has to be selected in the bottom field by means of the “Select” button.

Since the connection GUI is similar for all connectors other objects and connectors can also be selected among all objects and connectors present in the system.



1.2 Connection via Flexible Coupling

The GUI for flexible couplings is shown in figure 1.4. It has the new button “add Flexible Coupling Connection”, which opens the connection GUI shown in figure 1.5. The GUI now has the flexible coupling as default connector.

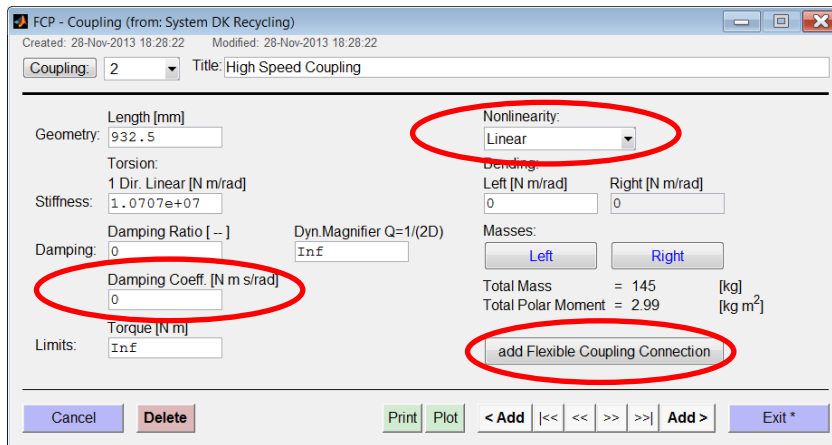


Fig. 1.4: Flexible Coupling GUI

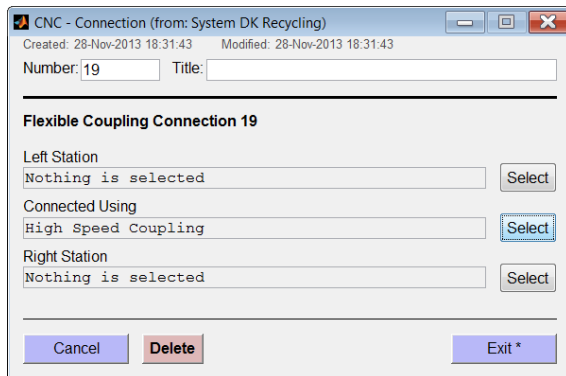


Fig. 1.5: Connection GUI called from flexible coupling

New features of the flexible coupling are nonlinear characteristics (see chapter 5) and the definition of a dimensioned damping coefficient (see chapter 11.2).



2. New Gear Connection Facilitating Double Meshes and Inner Meshes

As explained in chapter 1 the gear must be understood as a connector between shafts. This is different from previous versions, where the gear also contained the shafts. The shafts now must be part of the system in order to connect them to a gear via the gear meshes.

The new GUI for the gear is shown in figure 2.1. In this window the wheel mesh properties are defined. It has almost the same appearance as the GUI of previous versions with the following differences:

- The mesh type can be defined. Options are inner and outer mesh. In previous versions all meshes were outer meshes.
- There are no controls to add the wheel shaft, which is no longer part of the gear.

Clicking on the “Pinion” button opens a GUI for the parameters of the pinion mesh (see figure 2.2). Several pinions can be added to the gear.

The “Gear Connection” button opens a GUI to select the shafts (see figure 2.3). The field in the middle contains the gear. The wheel shaft, the pinion shaft and their stations for the mesh can be selected from menus, which can be opened with the select button next to the respective fields. The pinion and wheel can be selected among all shafts in the system.

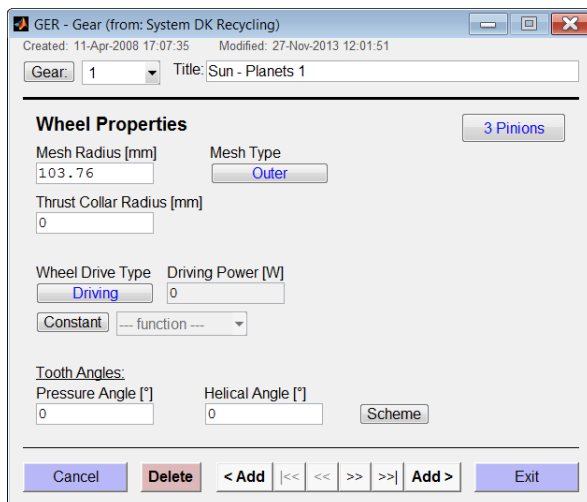


Fig. 2.1: Gear GUI

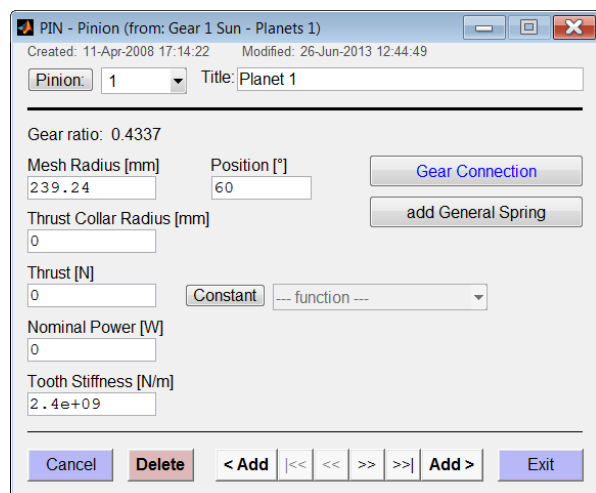
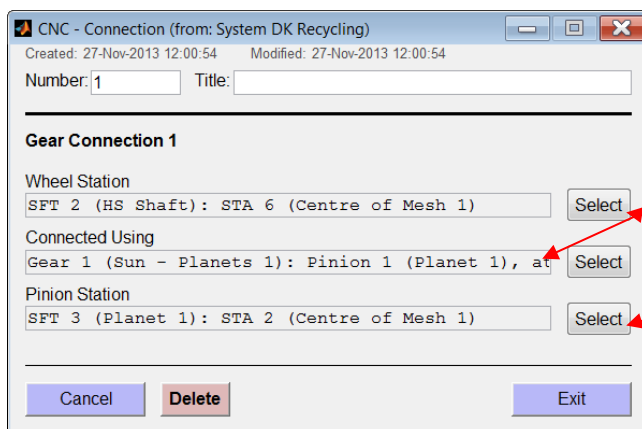


Fig. 2.2: Pinion GUI



Wheel and pinion is shown if called from pinion GUI

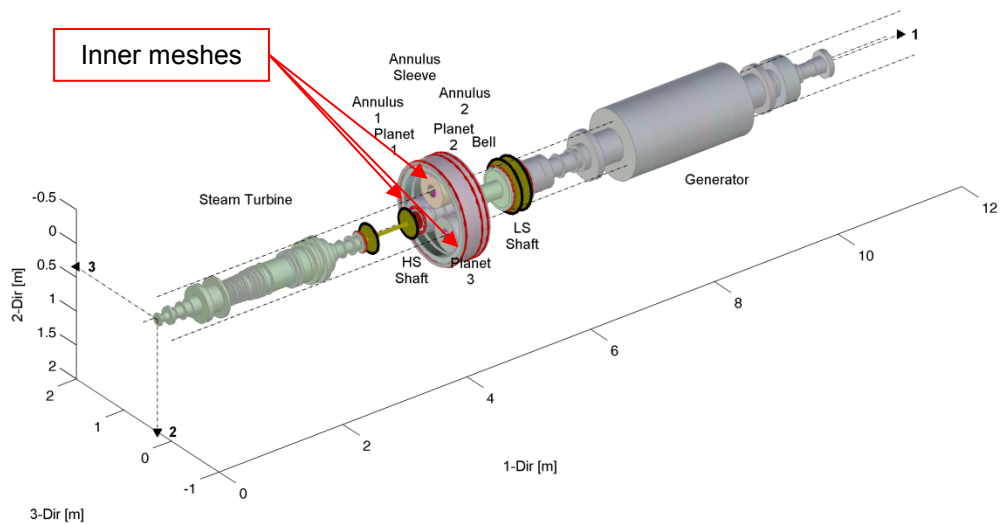
Shafts to be selected among shafts in the system

Fig.2.3: Gear connection GUI



In figure 2.4 the plot of a system with planetary gear is shown. The geometric correct modelling of the planetary gear is facilitated by the new feature “inner mesh”. This type of mesh is between the planets and the annulus.

Since the meshes are now separated from the shafts it is much easier to model double meshes. In the previous version each gear had one wheel mesh, one wheel shaft and at least one pinion. To create a double mesh it was necessary to separate the wheel and the pinions into two halves. This is no longer the case since the same pinion and wheel can be selected for different meshes.



MADYN 2000 v.3.8.development

Fig. 2.4: 3D plot of a system with planetary gear.



3. New Connection Facilitating Rotating Planets of Planetary Gears

Planets with a rotating axis have a rotating planet carrier. The planet carrier therefore has to be modelled as a rotor and connected to the planets or the planet axes, respectively. For this connection the new type of connector “Planet Carrier” is introduced. It can be added to a system from the system GUI with the help of the button “add Planet Carrier” (see figure 1.1).

The GUI of the planet carrier is shown in figure 3.1. The bolt circle diameter and a connection type can be defined. The connection GUI to connect planets or planet axes and the rotating planet carrier can be called as for other connectors from the connector GUI (see the button in figure 3.1), the station GUI or the system GUI.

In figure 3.2 a system with planets and rotors, which function as planet carrier, is shown. In case of a fixed planet, the planet carriers are not needed, since the planets can be fixed to the ground or some support model.

The carrier can be connected either directly to a rotating planet or to a fixed pin. In the latter case the actual planet has to be connected to the pin with a shaft in shaft connection (see chapter 4). The connection to the planet carrier is like a rigid connection, except for the rotation about the planet axis, which is free in case of a connection to a planet. In case of a connection to a pin the rotation of pin and carrier are equal.

It should be noted, that in case of a rotating planet carrier, the planets must be free in lateral direction, since rotation of the carrier causes a lateral movement due to the offset axes. This is illustrated in figure 3.3. In this figure the deformations are shown in case of a rotation of 1rad of the sun.

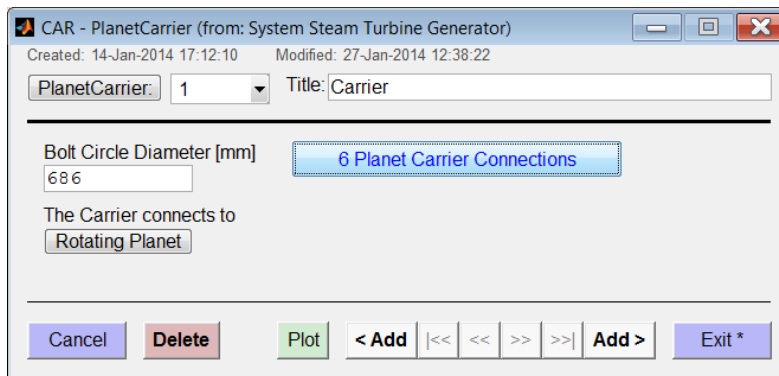


Fig. 3.1: GUI of the planet carrier



Steam Turbine Generator

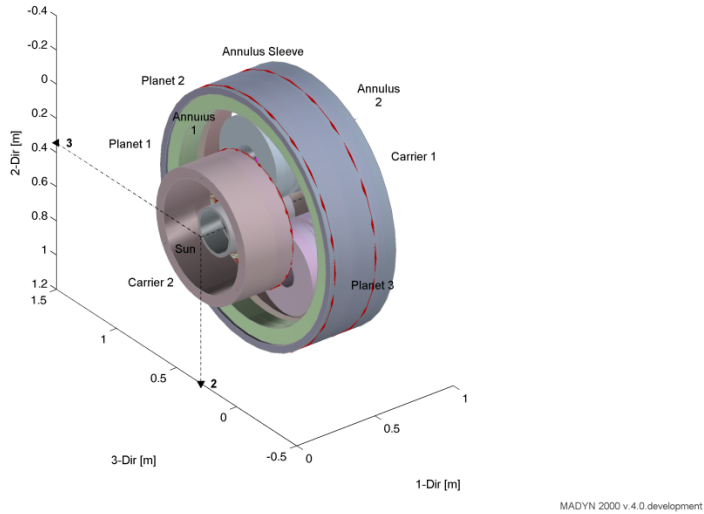


Fig. 3.2: Planetary gear with planet carrier.

Steam Turbine Generator

Static Analysis

Load case: StaticLC 1
 Analysis: 22-Jan-2014 18:28:25 - rel.speed=1
 Result Type: Displacements

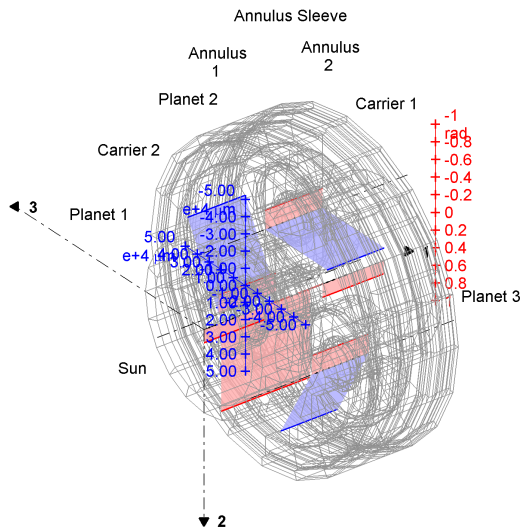
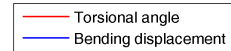


Fig. 3.3: Deformations of the planetary gear with rotating planets, for 1rad rotation of the sun



4. New Shaft in Shaft Connection via Radial Bearings

The connector for the shaft in shaft connection is an SBS (spring bearing support). The radial bearing connecting the two shafts is between the inner shaft and the SBS. Any radial bearing can be used for this connection. The outer shaft is radial rigidly connected to the SBS. The SBS GUI with the new connection button is shown in figure 4.1. The corresponding shaft in shaft connection GUI is shown in figure 4.2.

It should be noted, that SBS, which are used as connector must have zero damping and stiffness. Otherwise an error message appears. The SBS mass can be used and must not be zero, since normal SBS require non-zero masses for a regular mass matrix. The SBS mass has the effect of a concentrated mass added to the outer rotor.

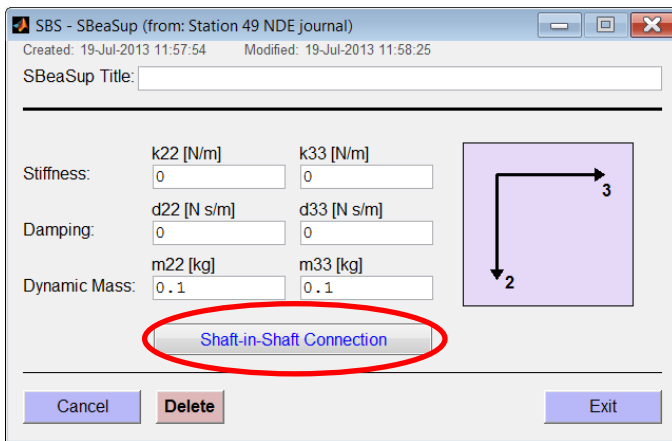


Fig. 4.1: SBS GUI with new connection button

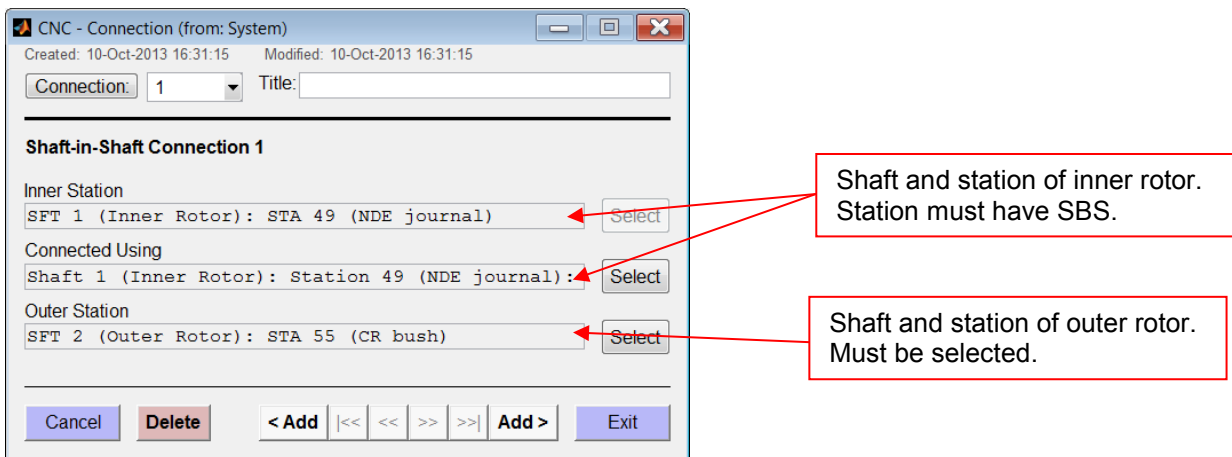


Fig. 4.2: Shaft in shaft connection GUI

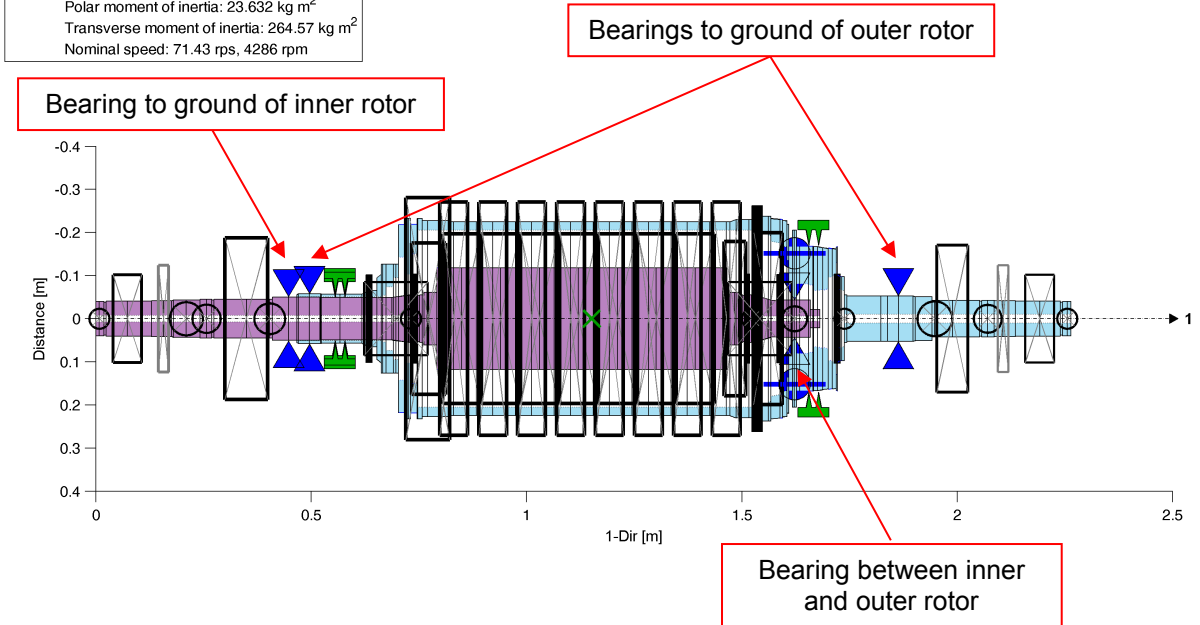
The plot of a system with an inner shaft, an outer shaft and a shaft in shaft connection via a bearing is shown in figure 4.3.



- 10 -

✕ Total mass: 1123.5 kg, CoG: 1151 mm
Polar moment of inertia: 23.632 kg m²
Transverse moment of inertia: 264.57 kg m²
Nominal speed: 71.43 rps, 4286 rpm

Inner Rotor, Outer Rotor



MADYN 2000 v.3.8.development

Fig. 4.3: System with a shaft in shaft connection via a bearing



5. New Nonlinear Capabilities

5.1 Flexible Coupling Nonlinearities: Rubber Coupling and Slipping Coupling

The flexible coupling GUI with the available non-linearities “Rubber Coupling” and “Slipping Coupling” is shown in figure 5.1. Both coupling types are quite common. Rubber couplings are used for their damping capabilities in case high response torques in resonances are expected as they can occur during an asynchronous run up of a synchronous motor. Slipping couplings are used to limit the torques in failure load cases such as short circuits.

The parameters for the non-linear functions can be defined in a window opened by the button “NL Function...”.

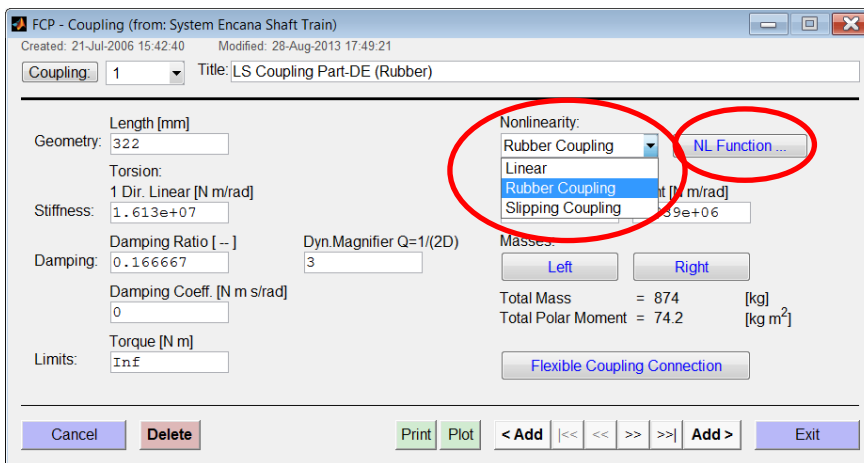


Fig. 5.1: Flexible coupling GUI with available non-linearities

The window to define the non-linear function for the rubber coupling can be seen in figure 5.2. It has a button to select a file with the characteristics and a button to plot it. The file to define the characteristic has to contain two columns with the angle in [°] and the moment in [Nm] as shown in table 5.1. The corresponding plot can be seen in figure 5.3. The characteristic only has to be defined for positive angles. The function then is mirrored at the zero point for negative angles.

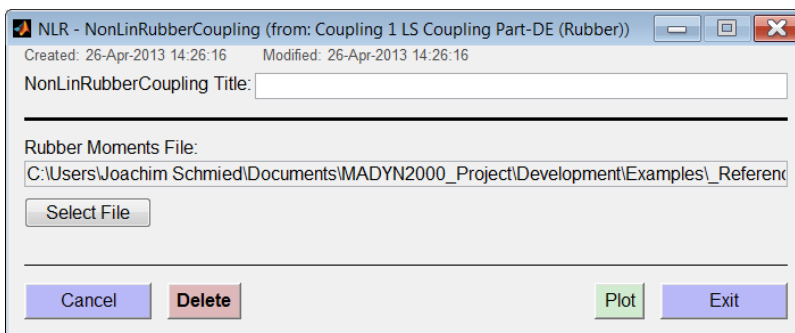


Fig. 5.2: GUI to define the non-linear function of the rubber coupling



Table 5.1: Content of the text file to define the non-linear function of the rubber coupling (1st column angle in [°], 2nd column moment in [Nm])

0	0
0.046	5107.6
0.092	10226.5
0.138	15368
0.184	20453
0.228	25538
0.271	30623
0.312	35821
0.351	40906
0.387	45991
0.42	51076
0.449	56274
0.476	61359
0.499	66444
0.519	71529
0.537	76727
0.553	81812
0.566	86897
0.579	91982
0.589	97180
0.599	102265
0.607	107350
0.615	112435
0.621	117520
0.627	123170
0.633	127690
0.637	133340
0.642	137860
0.645	143510
0.649	148030
0.652	153680
0.655	158200
0.657	163850
0.66	168370
0.662	174020
0.664	178540
0.666	184190
0.668	188710
0.669	194360
0.671	198880
0.672	204530

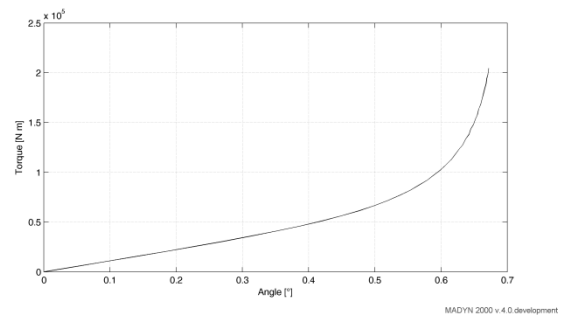
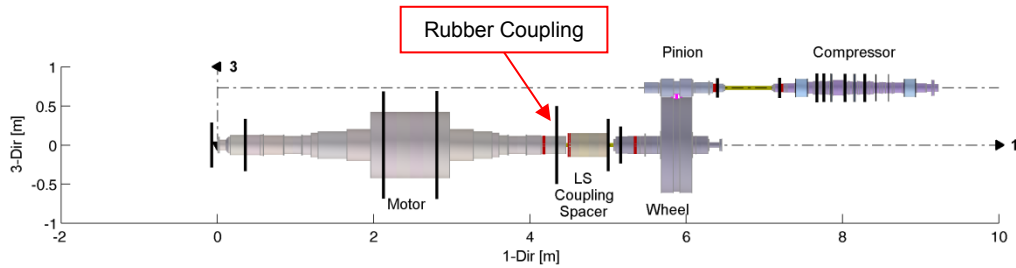


Fig. 5.3: Plot of the rubber coupling characteristic

The transient analysis has to be carried out with the modes of a linear coupling characteristic, which should be close to the linearised stiffness of the rubber coupling at the operating point. In figure 5.5 the coupling torque of the rubber coupling during an asynchronous run up with a synchronous motor is shown using the linear and non-linear characteristic. The system is shown in figure 5.4.



Shaft Train



MADYN 2000 v.3.8.development

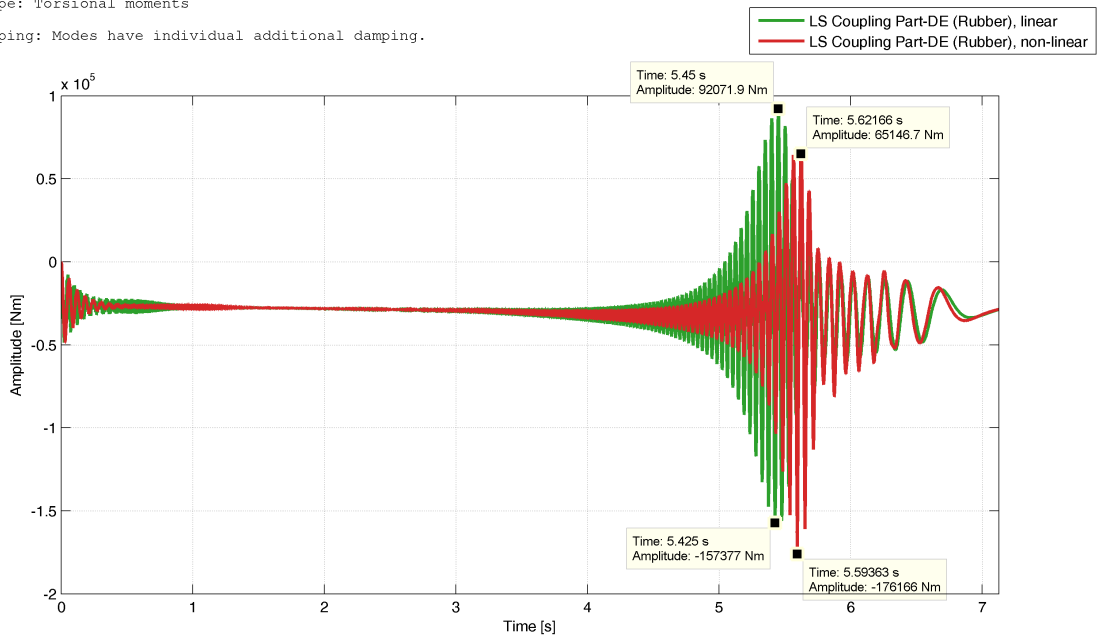
Fig. 5.4: System with rubber coupling

Shaft Train

Transient Response Analysis

Load case: TransientForceN 1 (Run Up)
 Analysis: 28-Aug-2013 18:53:51 - f(n), (Run up, linear,modes & damp- as in ref.) rel.speed=0, zero init.cond.
 Result Type: Torsional moments

Modal Damping: Modes have individual additional damping.



MADYN 2000 v.3.8.development

Fig. 5.5: Torque in the rubber coupling during an asynchronous run up with linear and non.linear rubber coupling characteristic

The GUI to define parameters for the slipping coupling is shown in figure 4.6. There are only two parameters, the slipping moment (sliding friction) and the initial slipping moment (sticking friction). A plot of the characteristic is shown in figure 5.7. As long as the coupling does not slip the linear torsional stiffness applies.

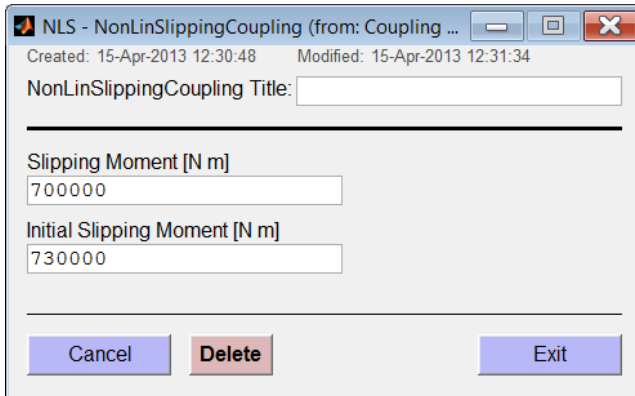


Fig.5.6: GUI to define the parameters of a slipping coupling

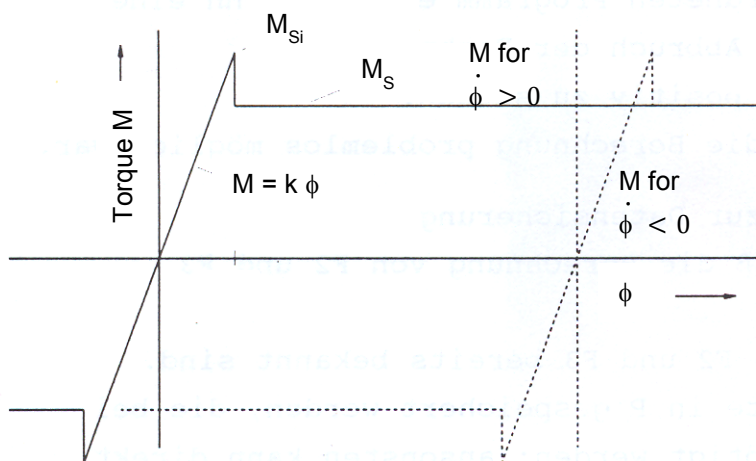
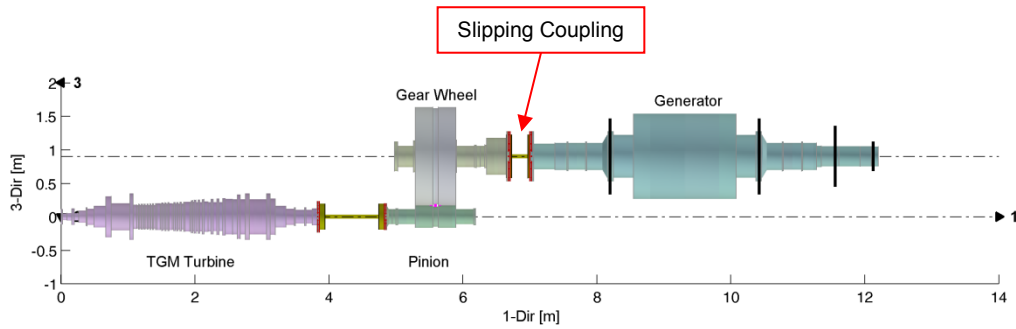


Fig. 5.7: Characteristic of the slipping coupling

For the system shown in figure 5.8 the short circuit response in the couplings is plotted in figure 5.9 for a non-slipping (linear) and slipping LS coupling. The effect of the slipping reducing the moment can be clearly seen. In figure 5.10 and 5.11 the response in the couplings for a mis-synchronisation with much higher torques is shown for a non-slipping and slipping coupling. In this case of the non-slipping linear coupling the maximum torque in the low speed coupling is three times higher than the slipping torque. The response torque with slipping then is completely different.



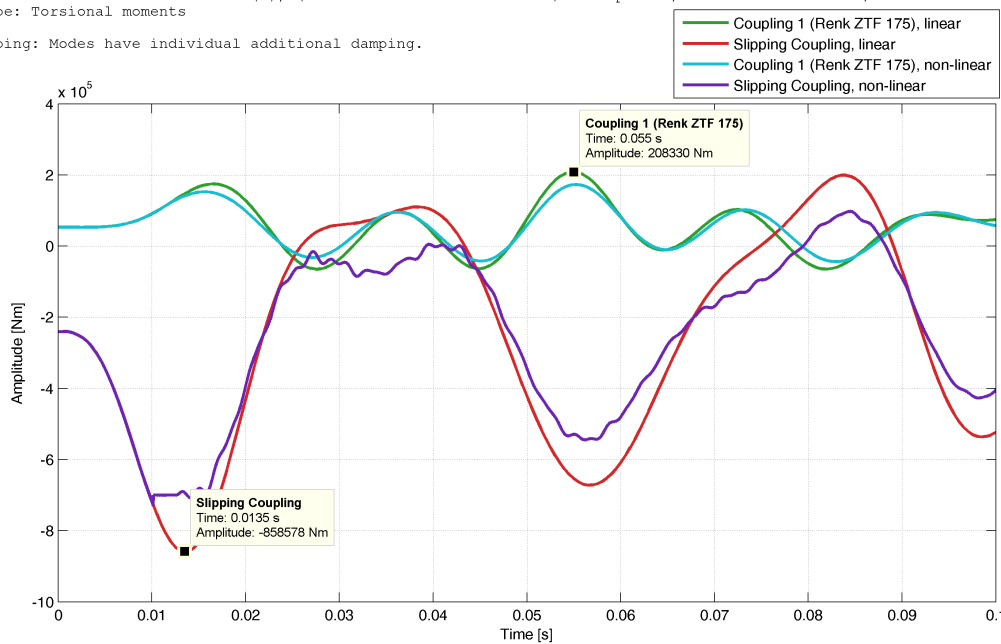
MADYN 2000 v.3.8.development

Fig. 5.8: System with slipping coupling

Transient Response Analysis

Load case: TransientForceT 4 (3-Phase Short Circuit (+))
 Analysis: 12-Feb-2013 18:33:41 - f(t), (Short Circuits from Preload) rel.speed=0, init.cond. from TRA, fluids deact.
 Result Type: Torsional moments

Modal Damping: Modes have individual additional damping.



MADYN 2000 v.3.8.development

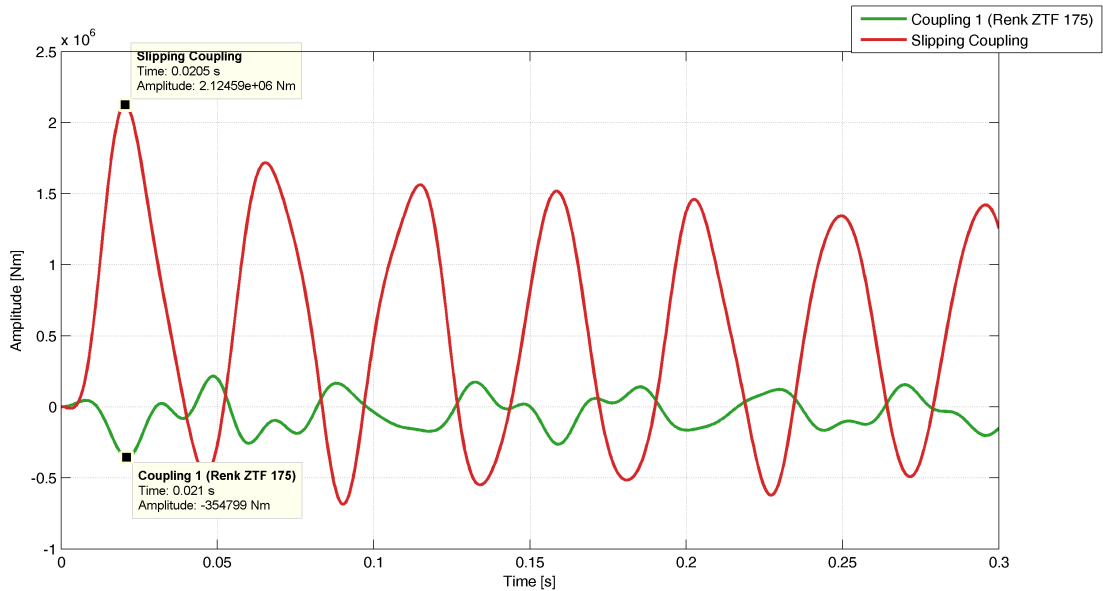
Fig. 5.9: Short circuit response of the system with non-slipping and slipping LS coupling



Transient Response Analysis

Load case: TransientForceT 6 (Synchronisation out of Phase)
Analysis: 16-Apr-2013 13:47:47 - f(t), (Mis-Synchronisation) rel.speed=0, zero init.cond., fluids deact.
Result Type: Torsional moments

Add. Modal Damping (all modes): 0.625 %



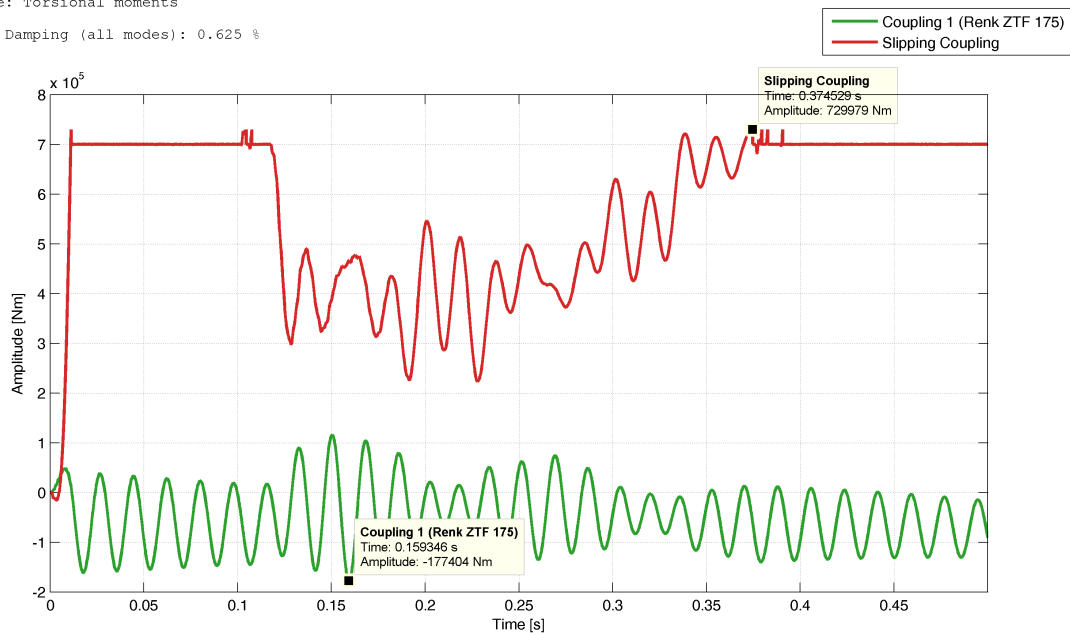
MADYN 2000 v.3.8.development

Fig. 5.10: Short circuit response of the system with non-slipping LS coupling

Transient Response Analysis

Load case: TransientForceT 6 (Synchronisation out of Phase)
Analysis: 02-Sep-2013 18:46:32 - f(t), (Mis-Synchronisation, nonlinear) rel.speed=0, zero init.cond., nonlinear, fluids deact.
Result Type: Torsional moments

Add. Modal Damping (all modes): 0.625 %



MADYN 2000 v.3.8.development

Fig. 5.11: Response to mis-synchronisation of the system with slipping LS coupling



5.2 General Nonlinearities

General nonlinear functions can be programmed using MATLAB code and coordinates of BBSs (black box shafts). The displacement/rotations (coordinates 1-3/4-6) and their velocities of any node in the BBS can be used to calculate forces, which are applied to any coordinate of the BBS. As explained in the documentation or in chapter 3 of the release note of version 3.7 (http://www.delta-js.ch/cms/upload/pdf/english/release_notes/MADYN_2000_Release_37.pdf) BBSs are extensions of MADYN 2000 models using MADYN classic code. In the following the modelling of an auxiliary bearing for magnetic bearings is explained. The model corresponds to the model in http://www.delta-js.ch/cms/upload/pdf/english/technical-papers/Rotor_Dropped_into_Auxiliary_Bearings_1992.pdf.

The BBS for the auxiliary bearing is shown in figure 5.12. It has two sections i.e. three nodes (#STA1 to #STA3). Only coordinate 3 is used for #STA2 and #STA3. These two nodes represent the inner race of the ball bearing and the coordinate 3 the ring rotation. The two stations are connected with a stiff spring and a mass is added to them representing the polar moment of inertia. #STA1 of the BBS is rigidly connected to the shaft, i.e. it functions like a shaft node.

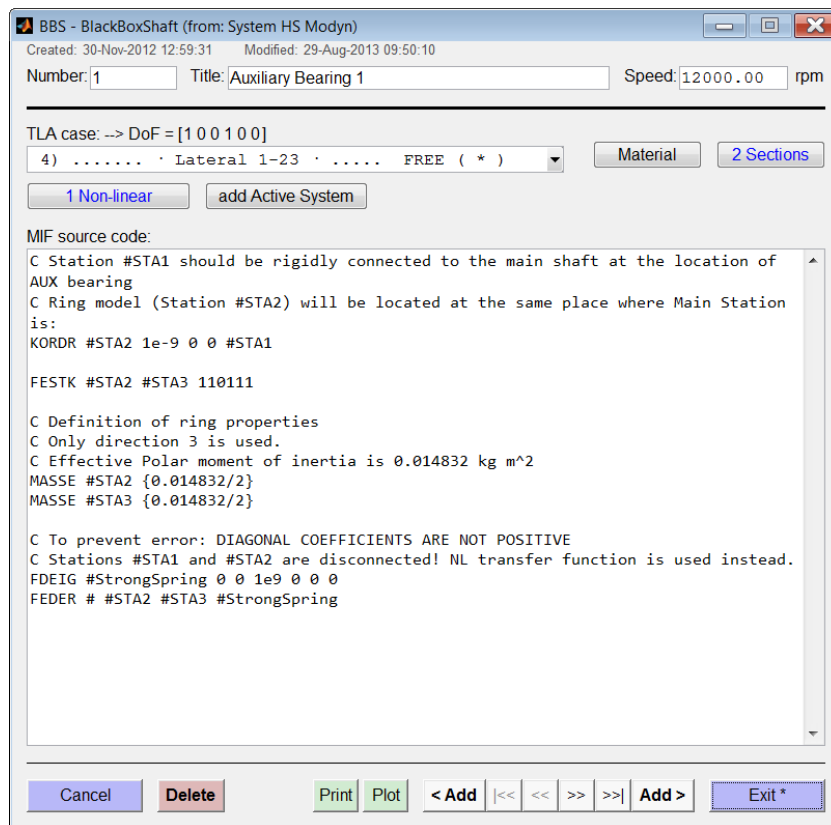


Fig. 5.12: BBS for auxiliary bearing

The window to define the function for the nonlinear force in MATLAB code using the BBS coordinates is shown in figure 5.13a. Parameters of the functions are displacements and velocities of the BBS coordinates, time and the relative shaft speed of the BBS. In the window the coordinates (station + direction), which are used by the function are defined.



Created: 18-Jul-2012 10:04:16 Modified: 30-Nov-2012 15:01:43

NonLinearFunc Title: _____

```

force = function(time, speedRel, displacements, velocities)
    Ft = 0;

    elseif oRace + 1e-3 < oRotor
        Ft = Fdt + mu*Fr; % Fr negative!

    else
        Ft = Fdt;
    end

    % M: Force on ring
    if oRace + 1e-3 < oRotor
        M = -R * mu * Fr;
    else
        M = 0;
    end

    % translate Fr and Ft back to 2-3 coordinate system
    [forceR(1), forceR(2)] = pol2cart(alphaDispl, Fr);
    [forceT(1), forceT(2)] = pol2cart(alphaDispl+pi/2, Ft);

    force(1:2) = forceR + forceT;
    force(3) = M;

```

Station	Coordinate
Station 1 (Connection)	2
Station 1 (Connection)	3
Station 2 (Ring1)	3

Buttons: Add, Delete, Cancel, Delete, Exit

Annotations:

- Calculation of forces for selected coordinates.
- Selected coordinates, which are used in the function. Coordinates can be added and deleted by the respective buttons.

Fig. 5.13a: Window to define the non-linear function for BBS

```

% r: rotor displacement
[alphaDispl,r] = cart2pol(displacements(1), displacements(2));
[alphaVel ,v] = cart2pol( velocities(1), velocities(2));

% angle between velocity and displacement
alpha = alphaVel - alphaDispl; % toDo: need to check coordinate
trnaformation

oRotor = speedRel * 200 * 2*pi; % Hz -> radians per second
oRace = velocities(3);

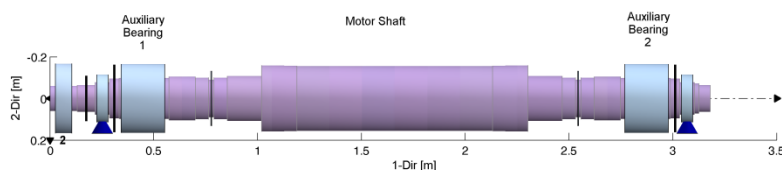
```

Annotations:

- Use of selected coordinates and relative speed in the code.

Fig. 5.13b: Part of the non-linear function code

Results of a drop analysis of the system in figure 5.14 can be seen in figure 5.15 to 5.18.



MADYN 2000 v.3.8.development

Figure 5.14: System with auxiliary bearings

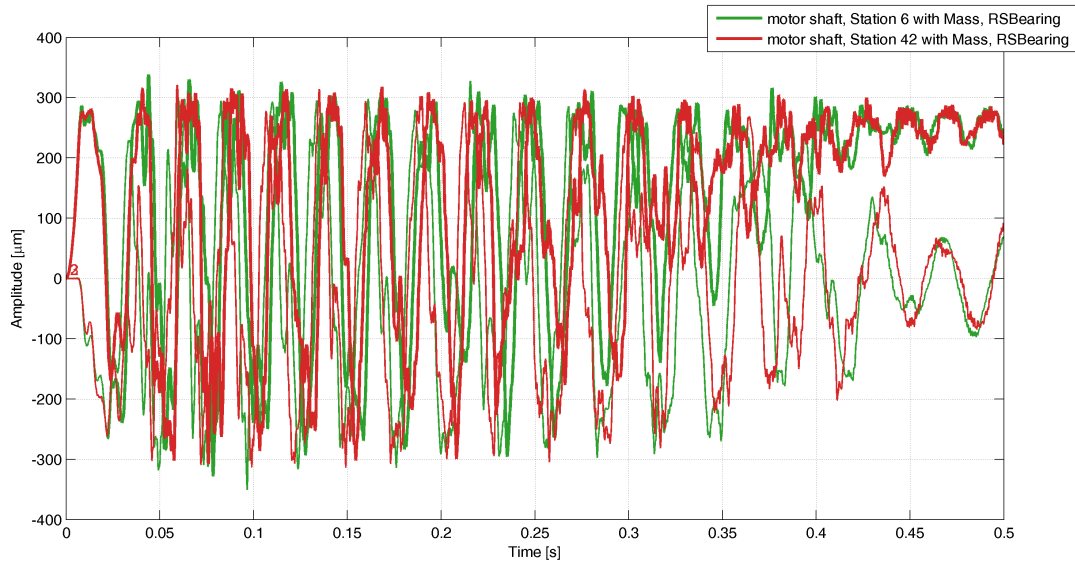


Transient Response Analysis

Load case: TransientBaseAcc 1
Analysis: 29-Aug-2013 09:53:22 - f(t), rel.speed=1.083, zero init.cond., nonlinear
Result Type: Bending displacement

Bold lines correspond to directions 2 and 2'

Add. Modal Damping (all modes): 0 %



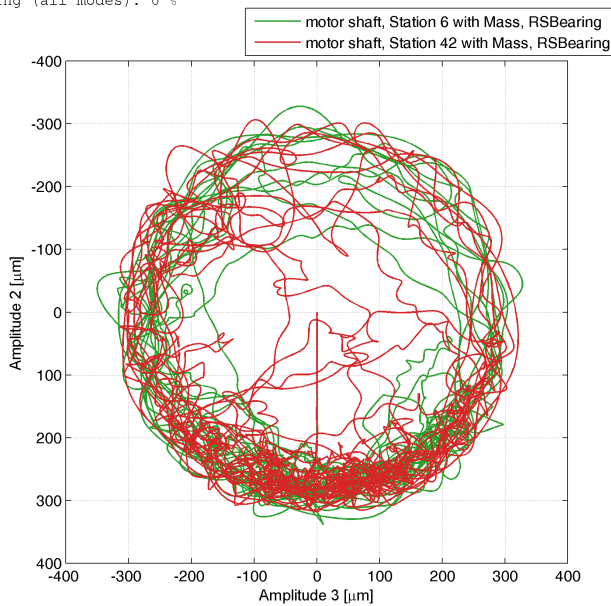
MADYN 2000 v.3.8.development

Fig. 5.15: Shaft displacements at the auxiliary bearings, drop at full speed

Transient Response Analysis

Load case: TransientBaseAcc 1
Analysis: 29-Aug-2013 09:53:22 - f(t), rel.speed=1.083, zero init.cond., nonlinear
Result Type: Bending displacement

Add. Modal Damping (all modes): 0 %



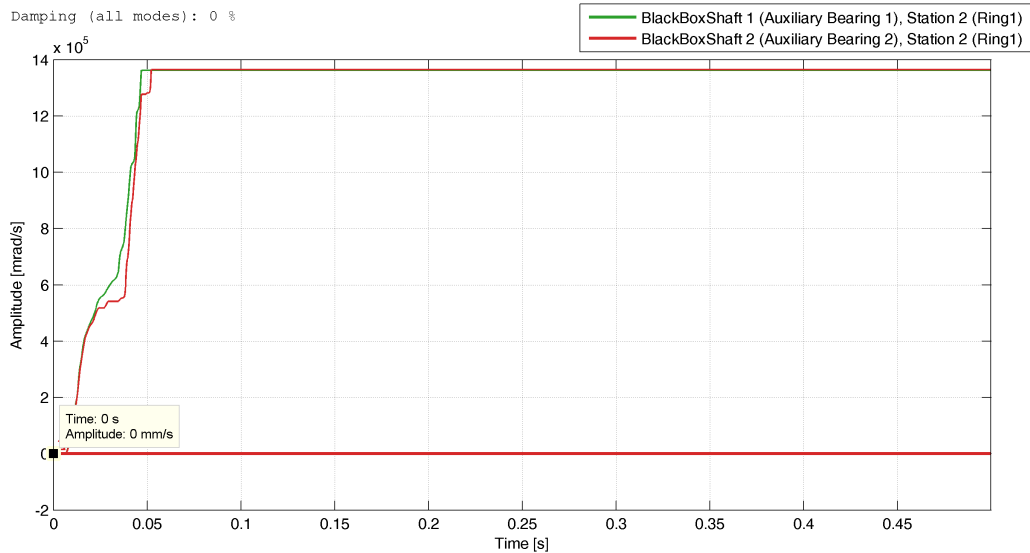
Time: from 0 to 0.5 s

MADYN 2000 v.3.8.development

Fig. 5.16: Orbit of shaft displacements at the auxiliary bearings, drop at full speed



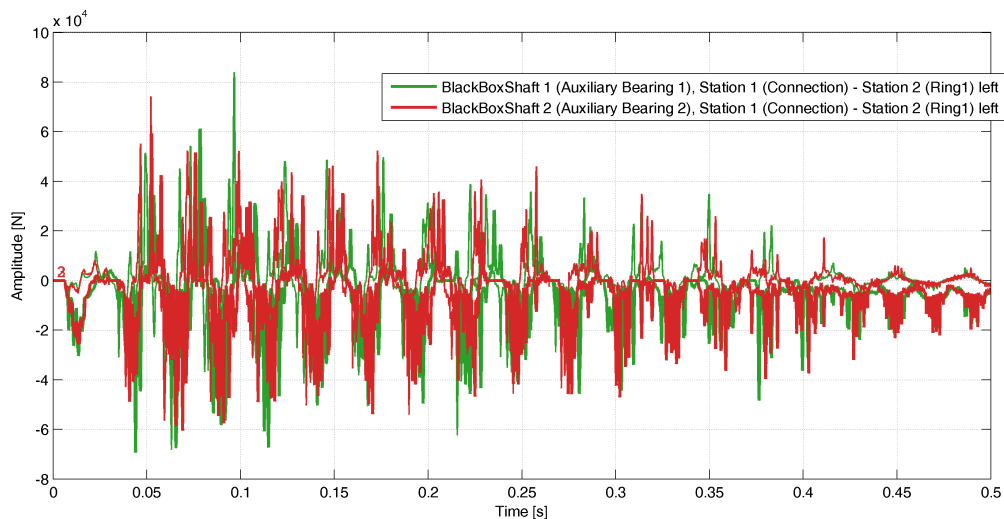
Transient Response Analysis
Load case: TransientBaseAcc 1 Bold lines correspond to directions 2 and 2'
Analysis: 29-Aug-2013 09:53:22 - f(t), rel.speed=1.083, zero init.cond., nonlinear
Result Type: Bending velocity
Add. Modal Damping (all modes): 0 %



MADYN 2000 v.3.8.development

Fig. 5.17: Ring speeds of the inner race of the auxiliary bearings, drop at full speed

Transient Response Analysis
Load case: TransientBaseAcc 1 Bold lines correspond to directions 2 and 2'
Analysis: 29-Aug-2013 09:53:22 - f(t), rel.speed=1.083, zero init.cond., nonlinear
Result Type: Bending forces
Add. Modal Damping (all modes): 0 %



MADYN 2000 v.3.8.development

Fig. 5.18: Auxiliary bearing forces, drop at full speed



6. Active Systems (apart from magnetic bearings)

“Axial Magnetic Bearings” and “Torsional Active Systems” were added as active systems in addition to the “Radial Magnetic Bearings”. The generic term for these systems is “Active System”. It is used in the GUIs instead “Radial Magnetic Bearings”.

6.1 Axial Magnetic Bearing

The “Active System GUI” with “Axial Magnetic Bearing” AMB selected among active systems is shown in figure 6.1. As direction only the axial direction is active. It cannot be selected. The GUI to create a controller from building blocks and to select the controller type can be opened in the same way by the button “Controller” as for radial magnetic bearings.

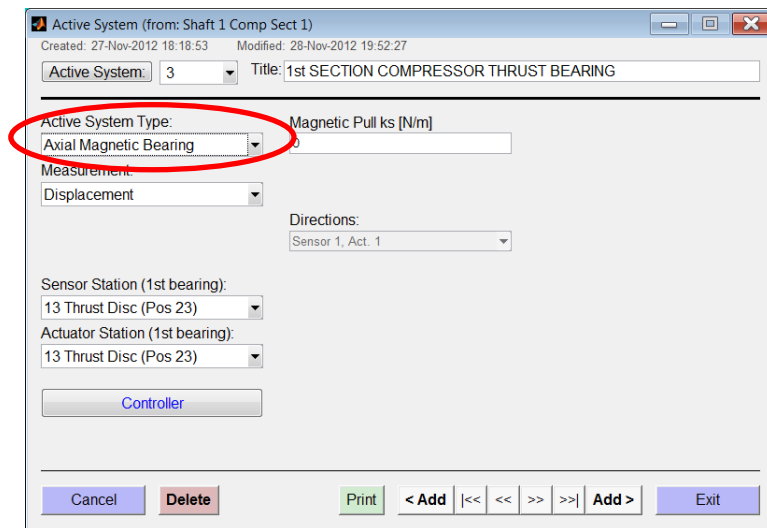
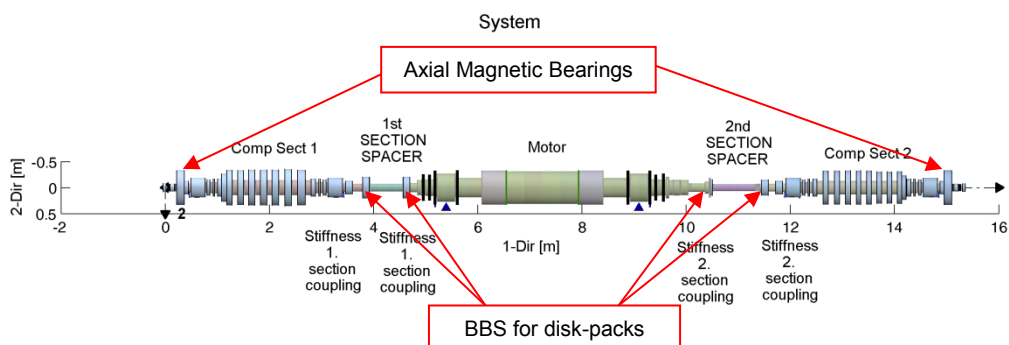


Fig. 6.1: Active system GUI for axial magnetic bearings

In figure 6.2 a system with axial magnetic bearing is shown. The system has flexible couplings, which are modelled with the spacers as shaft and the axial stiffness of the disk pack as black box shaft BBS. The two compressors with the new symbols for axial magnetic bearings are shown in figure 6.3.



MADYN 2000 v.3.8.development

Fig. 6.2: System with axial magnetic bearings



- 22 -

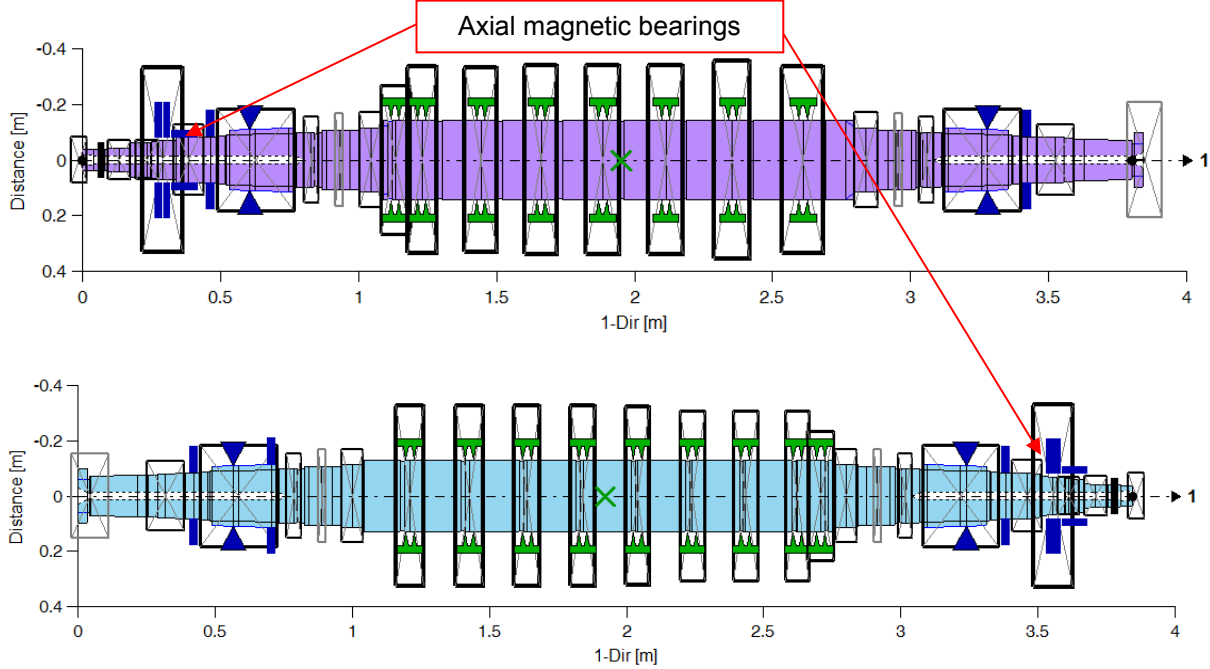


Fig. 6.3: Compressor shafts with axial magnetic bearings

The eigenvalues and natural modes of the system are shown in figure 6.4 and 6.5.

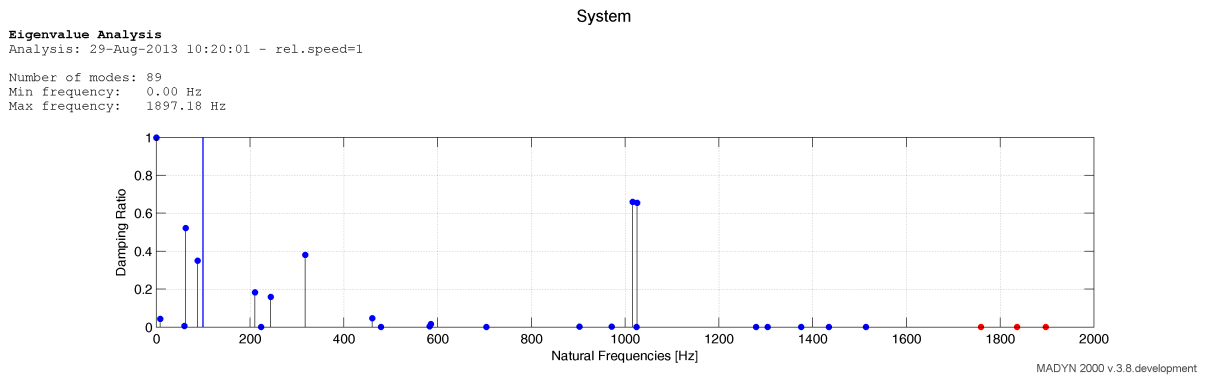


Fig. 6.4: Eigenvalues of the system with axial magnetic bearings

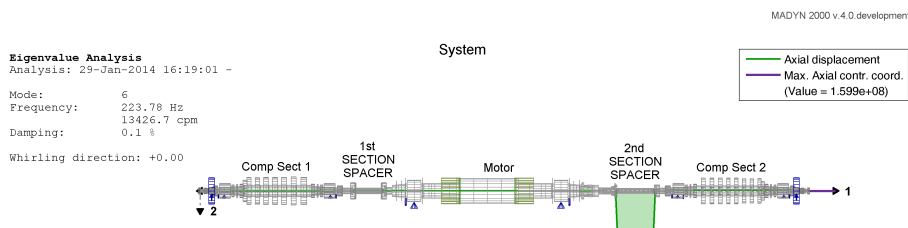
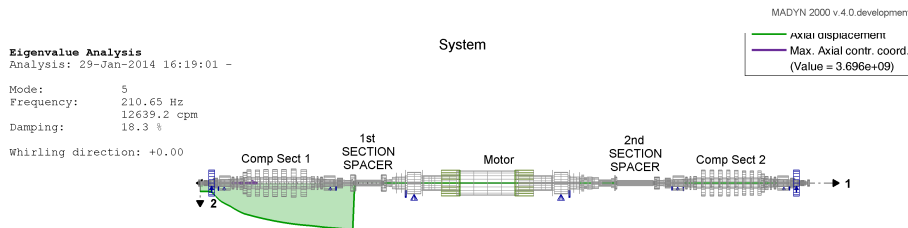
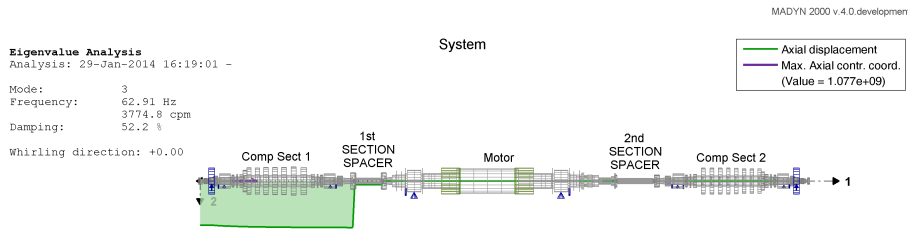
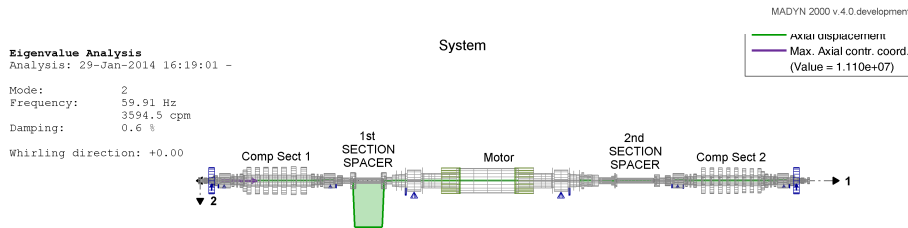
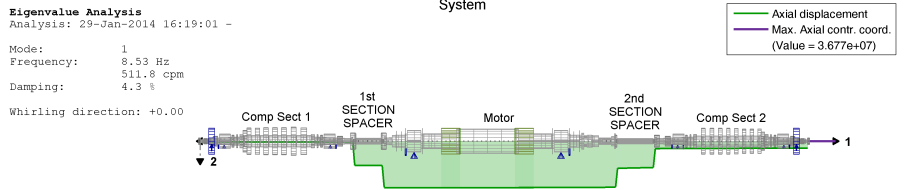


Fig. 6.5: Axial natural modes of the system with axial magnetic bearings



6.2 Active Torsional System

The “Active System GUI” with “Active Torsional System” ATS selected among active systems is shown in figure 6.6. As direction only the rotation about 1-direction (=direction 4) is active. It cannot be selected. The GUI to create a controller from building blocks and to select the controller type can be opened in the same way by the button “Controller” as for radial magnetic bearings.

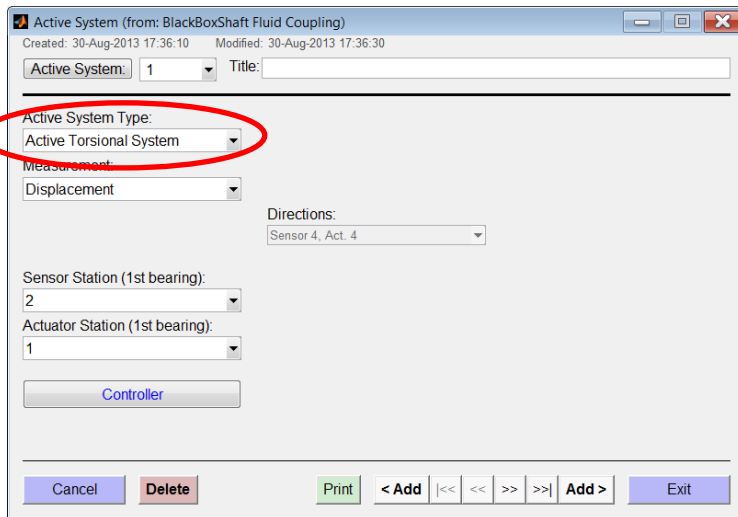
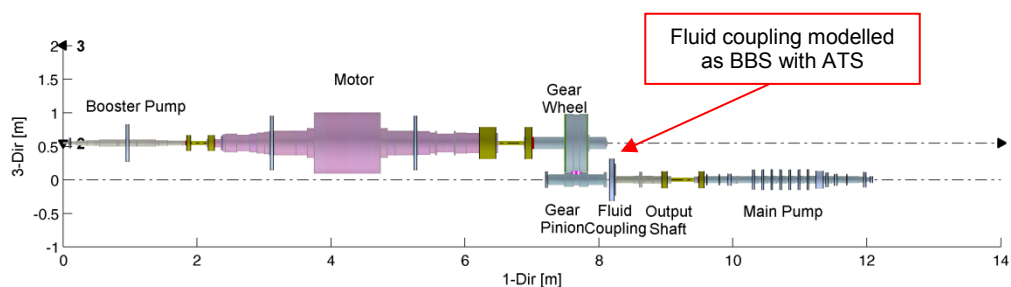


Fig. 6.6: Active system GUI for active torsional system

Active torsional systems can be used for example to model linear motor characteristics as a function of the shaft rotational speed. In the following an example to model the characteristic of a fluid coupling is described, which is a general transfer function. The system can be seen in figure 6.7, the transfer function of the fluid coupling describing the relation between angle and moment in figure 6.8. Since the input to a normal ATS is the absolute angle or angular velocity, a black box shaft BBS had to be used to create the relative displacement between the shaft ends of the pinion and output shaft by kinematic couplings in MADYN classic code. The coordinates in the BBS with the relative displacements (for the two shaft ends the relative displacements have different sign) are used as sensor and the connection nodes of the BBS to the pinion and output shaft as actuators applying the force.



MADYN 2000 v.3.8.development

Fig. 6.7: System with fluid coupling modelled as a black box shaft with active torsional system

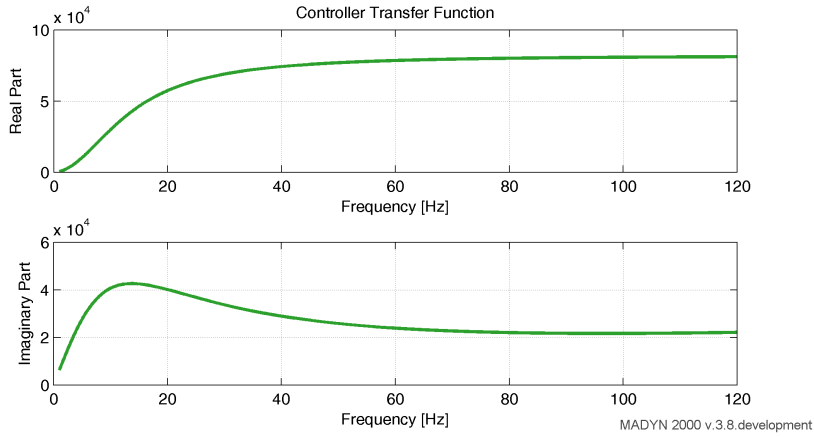


Fig. 6.8: Transfer function (real and imaginary part) of the fluid coupling, moment in Nm per angle

The eigenvalues and mode shapes for this system are shown in figure 6.9 and 6.10.

Eigenvalue Analysis
Analysis: 04-Sep-2013 17:20:46 - rel.speed=1
Number of modes: 83
Min frequency: 0.00 Hz
Max frequency: 9953.75 Hz

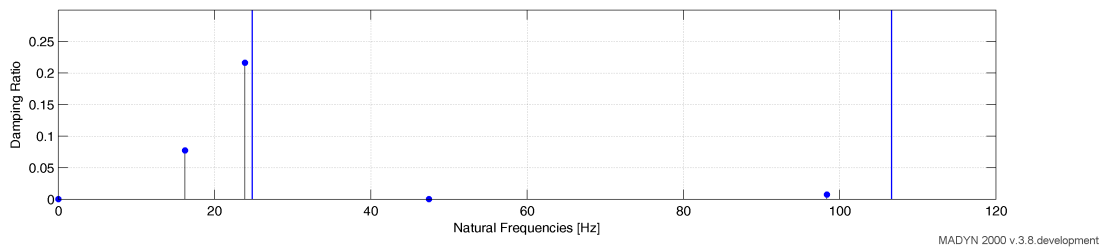


Fig. 6.9: Eigenvalues of the system with fluid coupling

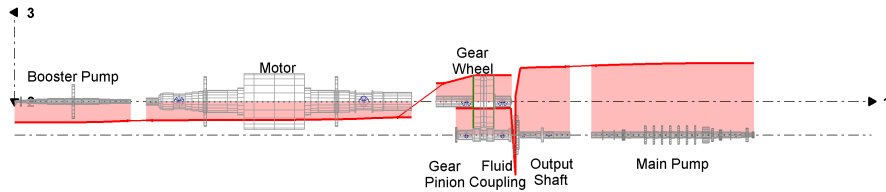


- 26 -

System

Eigenvalue Analysis
Analysis: 04-Sep-2013 17:20:46 -
Mode: 6
Frequency: 16.21 Hz
Damping: 972.4 cpm
7.7 %
Whirling direction: +0.00

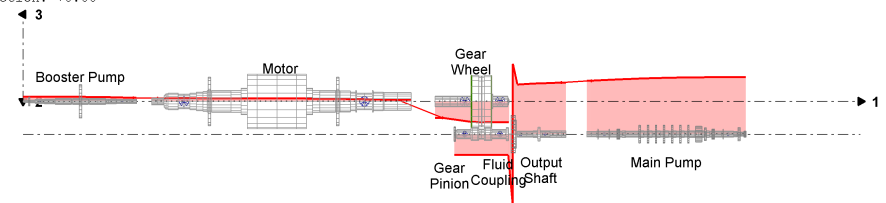
Torsional angle



System

Eigenvalue Analysis
Analysis: 04-Sep-2013 17:20:46 -
Mode: 7
Frequency: 23.89 Hz
Damping: 1433.2 cpm
21.6 %
Whirling direction: +0.00

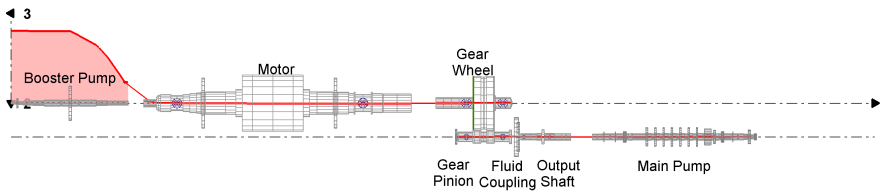
Torsional angle



System

Eigenvalue Analysis
Analysis: 04-Sep-2013 17:20:46 -
Mode: 8
Frequency: 47.45 Hz
Damping: 2846.9 cpm
0.0 %
Whirling direction: +0.00

Torsional angle



System

Eigenvalue Analysis
Analysis: 04-Sep-2013 17:20:46 -
Mode: 9
Frequency: 98.36 Hz
Damping: 5901.4 cpm
0.8 %
Whirling direction: +0.00

Torsional angle

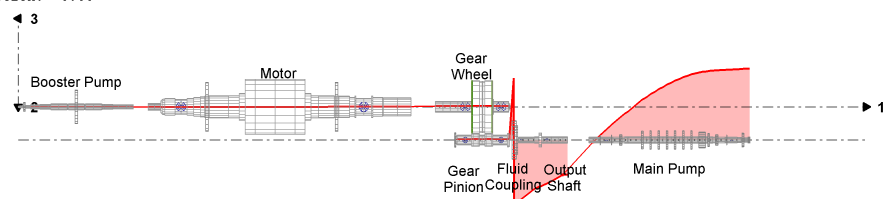


Fig. 6.10: Mode shapes of the system with fluid coupling



6.3 Imported Transfer Function in Table Form

Transfer functions of active systems may be given in table form as shown in the following:

Frequency	Stiffness	Damping
1.0	500.0	2000.0
2.0	2000.0	900.0
...		

The frequency must be given in Hz.

Alternatively to “Stiffness and Damping” values “Real and Imaginary” part or “Amplitude and Phase” may be listed.

All active systems now have the new building block “imported” allowing importing such a list as transfer function. The controller GUI with this building block is shown in figure 6.11. The button “Define Transfer Function” opens the window shown in figure 6.12 to select a file with the above described content and edit fields to define numerator and denominator polynomials.

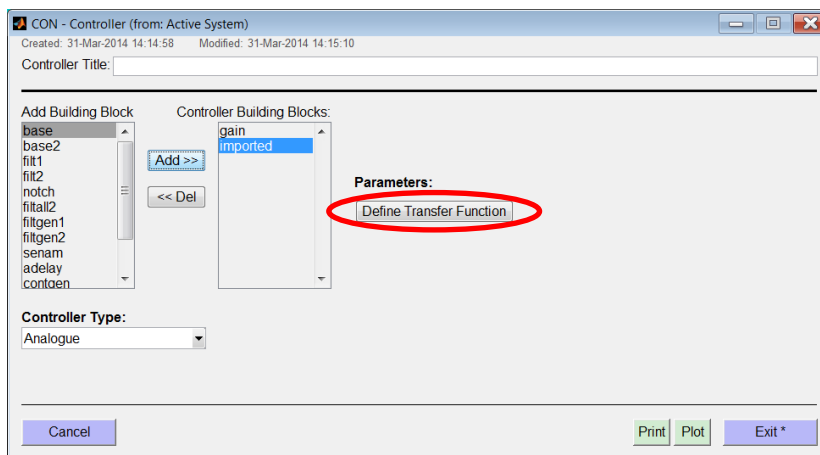


Fig. 6.11: Controller GUI with building block “imported”

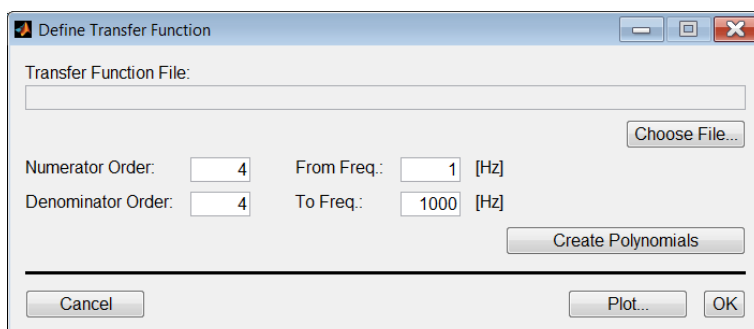


Fig. 6.12: Window to the define the imported transfer function

In the print of a controller with an imported transfer function the polynomials as well as the poles and zeros of the imported function are shown. The poles allow checking if the function is stable or not. In case a pole has positive real parts it is unstable and may cause instability of the system.



7. Rolling Element Bearings

In general rolling element bearings (REB) are speed dependent (considering the centrifugal and gyroscopic effect of the rolling elements, which can change the contact angles for some types of bearings) and the force displacement relation is nonlinear. The affected coordinates are the displacements in axial and radial direction x_1 , x_2 , x_3 and rotations about the radial axes Φ_2 , Φ_3 . In contrast to current radial bearings also the rotational coordinates around 2 and 3 as well as the axial displacement are involved. To calculate linear vibrations the concept of considering rolling elements is quite similar to fluid film bearings. The force displacement relationship can be linearized around the static equilibrium. The linearized behaviour can be described by a 5x5 speed dependent stiffness matrix $K(n)$. For the modelling of the bearing and analysis of the stiffness matrix software provided by MESYS is integrated into MADYN 2000 (see /1/).

The GUI to define rolling element bearings is shown in figure 7.1. A check box can be activated to consider the centrifugal force. For bearings, which can take radial and axial loads the boundary conditions "Axially loose" or "Axially fixed" can be selected. The "Edit Bearing" button opens the GUI in figure 7.2 of MESYS to define the bearing geometry, lubrication and material properties.



Fig. 7.1: GUI to define a rolling element bearing

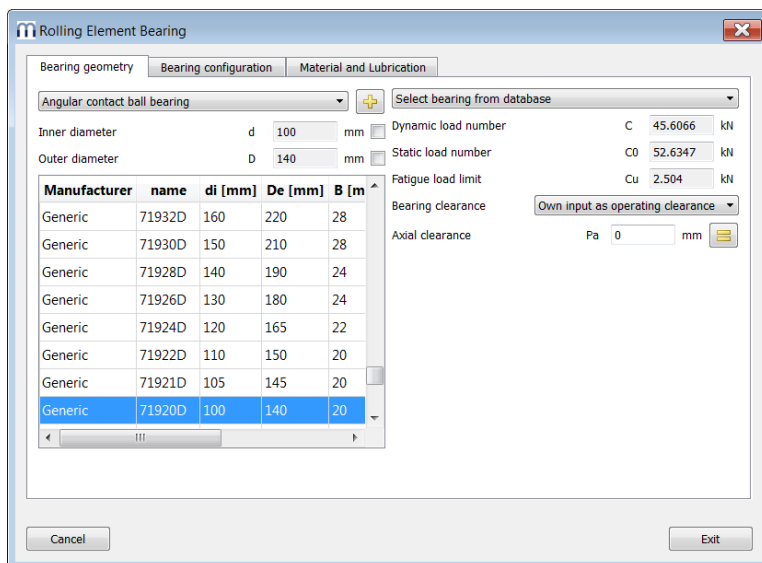


Fig. 7.2: MESYS GUI to define the bearing properties



The MESYS software has a database to select among different sizes and types of bearings. Alternatively the bearing geometry can be defined. In table 7.1 the available types of bearing and their boundary conditions are listed.

Table 7.1: Bearing types and their boundary conditions (loads they can take)

	Bearing Type	Boundary Conditions
1	Deep groove ball bearing	Load in radial and axial direction
2	Double deep groove ball bearing	Load in radial and axial direction
3	Axial deep groove ball bearing	Load in radial and axial direction, small radial load
4	Radial angular contact bearings	Load in radial and axial direction
5	Axial angular contact bearings	Load in radial and axial direction
6	Double row angular contact bearings	Load in radial and axial direction
7	Single row spherical ball bearings	Load in radial and axial direction (no moment)
8	Double row spherical ball bearings	Load in radial and axial direction (no moment)
9	Four point ball bearings considered as radial bearings	Load in radial and axial direction
10	Four point ball bearings considered as axial bearings	Load in radial and axial direction
11	Duplex ball bearings (double deep groove ball bearing with axial offset)	Load in radial and axial direction
12	Radial cylindrical roller bearings	Load in radial direction only (NU,N). Types with shoulder also in axial direction (NUP, NJ single direction).
13	Double row radial cylindrical roller bearings	Load in radial direction only. Types with shoulder also in axial direction.
14	Axial cylindrical roller bearings	Load in axial direction only
15	Needle bearings	Load in radial direction only
16	Taper roller bearings	Load in radial and axial direction. Axial load is necessary. Its magnitude can be estimated by setting $x1=0$.
17	Spherical roller bearings	Load in radial and axial direction (no moment)

The REB data can be exported to MESYS XML files and loaded from XML files by the context menu shown in figure 7.3, which is opened with a right mouse click in the GUI.

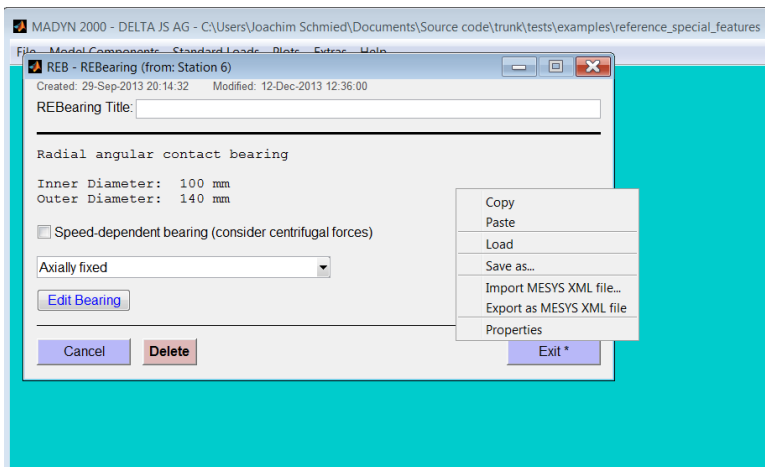
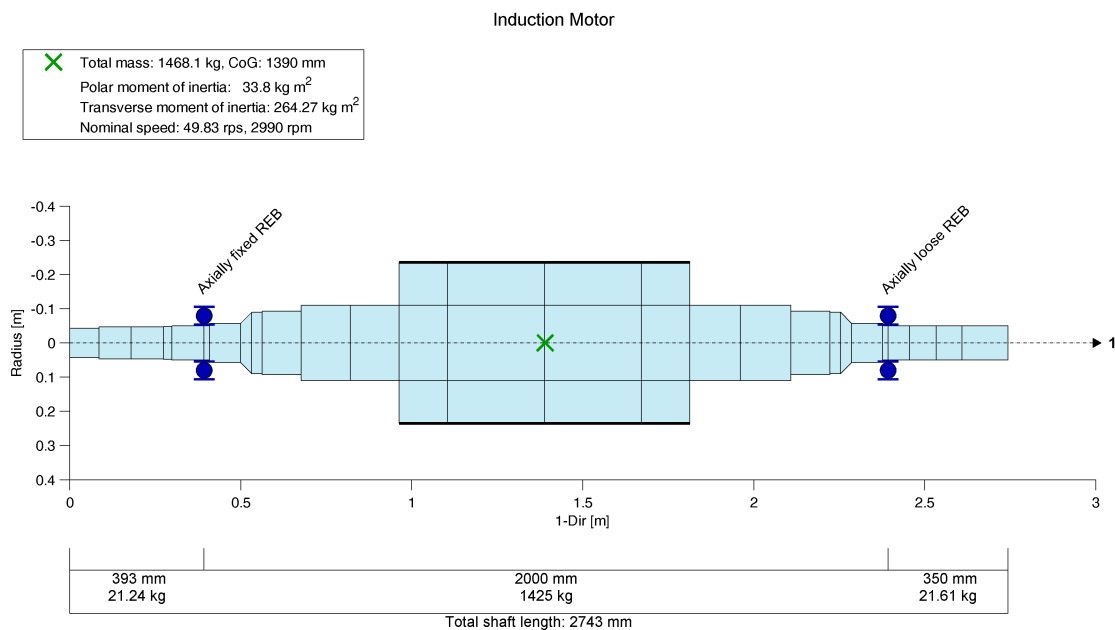


Fig. 7.3: Context menu to import and export MESYS XML files

In figure 7.4 a system of an induction motor with rolling element bearings is shown. The symbol for this new type of bearing can be recognised. The REB type in the system is an angular contact bearing, which can take axial and radial loads.



MADYN 2000 v.3.8.development

Fig. 7.4: System with REB

The static load for this system is shown in figure 7.5. The corresponding shaft deformation and shaft forces can be seen in figure 7.6 and 7.7 for a radial axial coupled analysis. A magnification of the bending moments at the axially fixed bearing can be seen in figure 7.8.



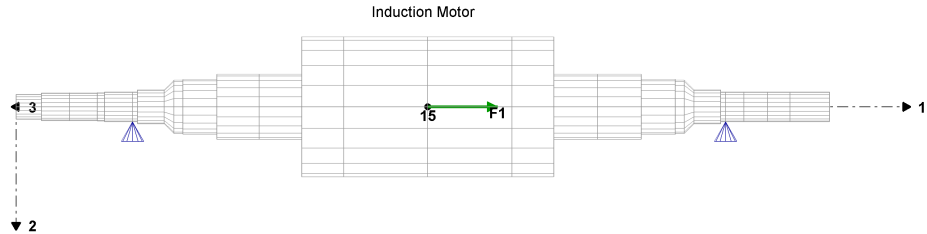
System Induction Motor

Static Loads

Load case: StaticLCCom 1 (Weight and Axial Bearing Forces)

Gravitation:

$$g_1 = 0.00 \text{ m/s}^2, g_2 = 9.81 \text{ m/s}^2, g_3 = 0.00 \text{ m/s}^2$$



Label Force 1-dir
F1 5000 N

MADYN 2000 v.3.8.development

Fig. 7.5: Loads for static analysis

System Induction Motor

Static Analysis

Load case: StaticLCCom 1 (Weight and Axial Bearing Forces)

Analysis: 02-Dec-2013 18:18:13 - rel.speed=1

Result Type: Displacements

— Bending displacement
— Axial displacement

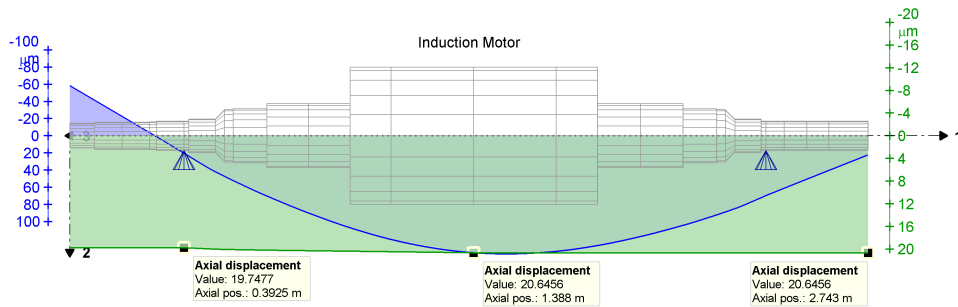


Fig. 7.6: Static deformation

System Induction Motor

Static Analysis

Load case: StaticLCCom 1 (Weight and Axial Bearing Forces)

Analysis: 02-Dec-2013 18:18:13 - rel.speed=1

Result Type: Forces and Moments

— Bending moments
— Shear forces
— Axial forces
— REB forces

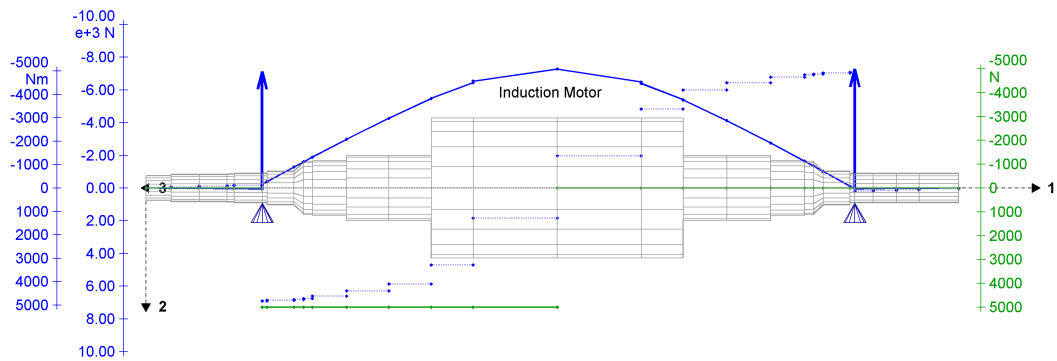


Fig.7.7: Static shaft forces

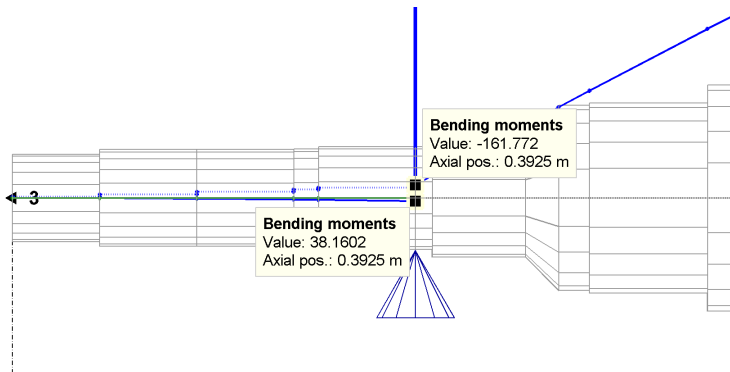


Fig. 7.8: Shaft bending moments at the axially fixed bearing

The main axial displacement takes place in the fixed bearing as can be seen in figure 7.6. The axial shaft deformation due to the axial shaft force is much smaller. In figure 7.8 can be recognised, that the angular contact bearing applies a moment of about 200Nm on the shaft (difference of 38N and -162N).

The stiffness matrices for this load can be seen in the following table.

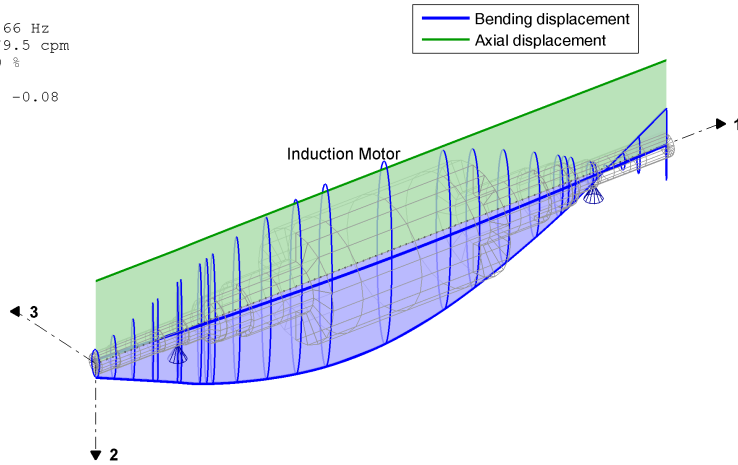
Table 7.2: Rolling element bearing stiffnesses

Rolling Element Bearing Properties:							
Induction Motor: Station 6 (Axially fixed REB)							
Station 6, General Stiffness Matrix:							
	k1	k2	k3	k4	k5	k6	
	[1/m]	[1/m]	[1/m]	[1/rad]	[1/rad]	[1/rad]	
[N]	244883690.9919	209604712.1856	-0.0016	0	-3.7783e-08	-6842.6132	
[N]	209598391.4818	442354558.3198	8.2423e-04	0	3.5758e-08	-12138.2273	
[N]	0.0012	-0.0038	499840938.8048	0	14764.3571	9.9050e-08	
[N m]	0	0	0	0	0	0	
[N m]	-5.2250e-05	-9.2768e-06	14757913.0320	0	484276.5381	1.6200e-07	
[N m]	-6833611.2173	-12135884.0467	-1.1233e-04	0	-3.3242e-06	397147.0856	
Station 6, General Damping Matrix is empty							
Induction Motor: Station 24 (Axially loose REB)							
Station 24, General Stiffness Matrix:							
	k1	k2	k3	k4	k5	k6	
	[1/m]	[1/m]	[1/m]	[1/rad]	[1/rad]	[1/rad]	
[N]	0	0	0	0	0	0	
[N]	0	460541004.6120	0.0036	0	-1.6513e-10	-49.2777	
[N]	0	-0.0042	110128058.8847	0	-6.9134	5.0506e-10	
[N m]	0	0	0	0	0	0	
[N m]	0	-3.1760e-04	-26768.1966	0	7614.3257	3.6664e-08	
[N m]	0	33781.2276	3.6671e-05	0	-7.6953e-09	52443.7659	
Station 24, General Damping Matrix is empty							

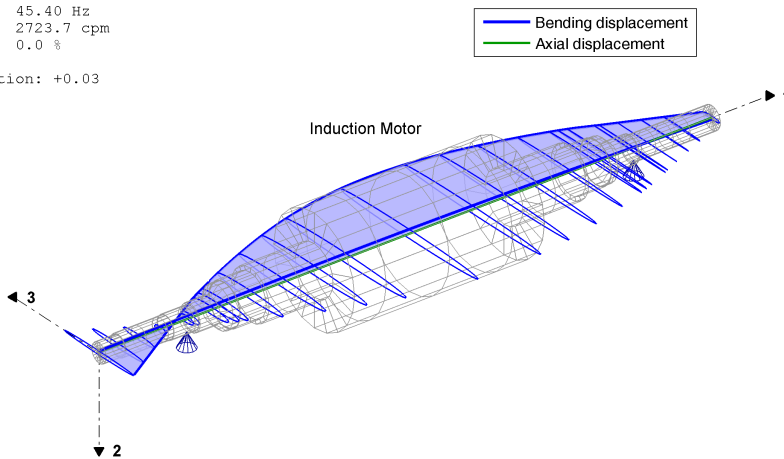
The natural modes of the shaft can be seen in figure 7.9. The coupling of axial and bending vibrations can be clearly seen. The vertical bending and axial direction couple in two modes with different direction of the axial vibration with respect to the bending direction.



Relative speed: 100%
Mode: 1
Frequency: 44.66 Hz
2679.5 cpm
Damping: 0.0 %
Whirling direction: -0.08



Relative speed: 100%
Mode: 2
Frequency: 45.40 Hz
2723.7 cpm
Damping: 0.0 %
Whirling direction: +0.03



Relative speed: 100%
Mode: 3
Frequency: 55.68 Hz
3341.0 cpm
Damping: 0.0 %
Whirling direction: +0.02

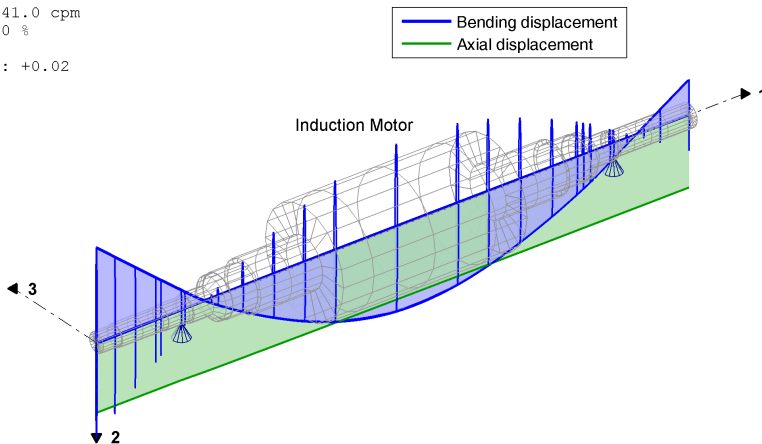


Fig. 7.9: Natural modes of the system with REB



8. Squeeze Film Damper (SFD)

8.1 Squeeze Film Damper in a Floating Ring Bearing

Setting the ring speed of a floating ring bearing to zero will create a squeeze film damper for the outer film. Squeeze film dampers are not able to carry a load unless the ring has a tangential velocity, which creates a radial force. Horizontal rotors with a weight therefore require an analysis considering the static and dynamic load simultaneously; they cannot be calculated separately and later superimposed, i.e. a nonlinear analysis is required. In case of a linear analysis the damping coefficients of the squeeze film damper in centred position are calculated.

The GUI of the floating ring bearing with zero ring speed is shown in figure 8.1. The button opening the outer bearing (Outer RFBearing) changes to “Outer SF-Damper” in case of zero ring speed. The GUI for the squeeze film damper is shown in figure 8.2.

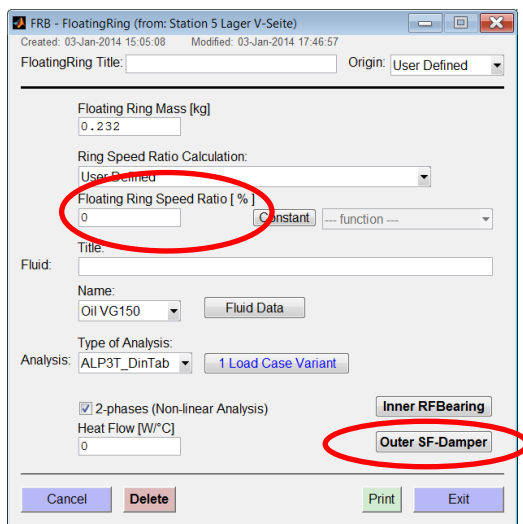


Fig. 8.1: FRB GUI with squeeze film damper

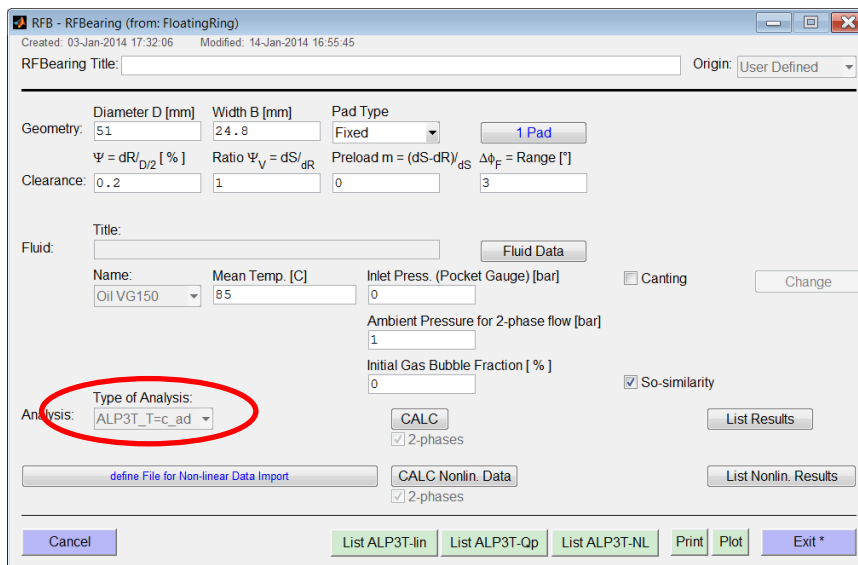


Fig. 8.2: GUI for the squeeze film damper



The GUI for the squeeze film damper is shown in figure 8.2. Only analysis type “ALP3T_T=c_ad” (constant adiabatic) with or without 2-phase flow, which is defined in the FRB GUI, are available. The analysis is carried out without turbulence (i.e. without Re-number). The load definition does not play a role, since only the centred position is analysed in case of the linear characteristics. Therefore only one set of dimensioned damping coefficients is shown under “List Results”. In the nonlinear characteristics the So-number and the α -angle are all zero, since the SFD cannot create a force caused by rotation. They are not shown under “List Results”. Two sets of damping coefficients β_{ik}^+ and β_{ik}^- are listed and can be plotted. The β_{ik}^+ values apply for a positive radial velocity (movement in direction of the bearing wall), whereas the β_{ik}^- values are used for negative radial velocity (movement away from the wall), see figure 8.3.

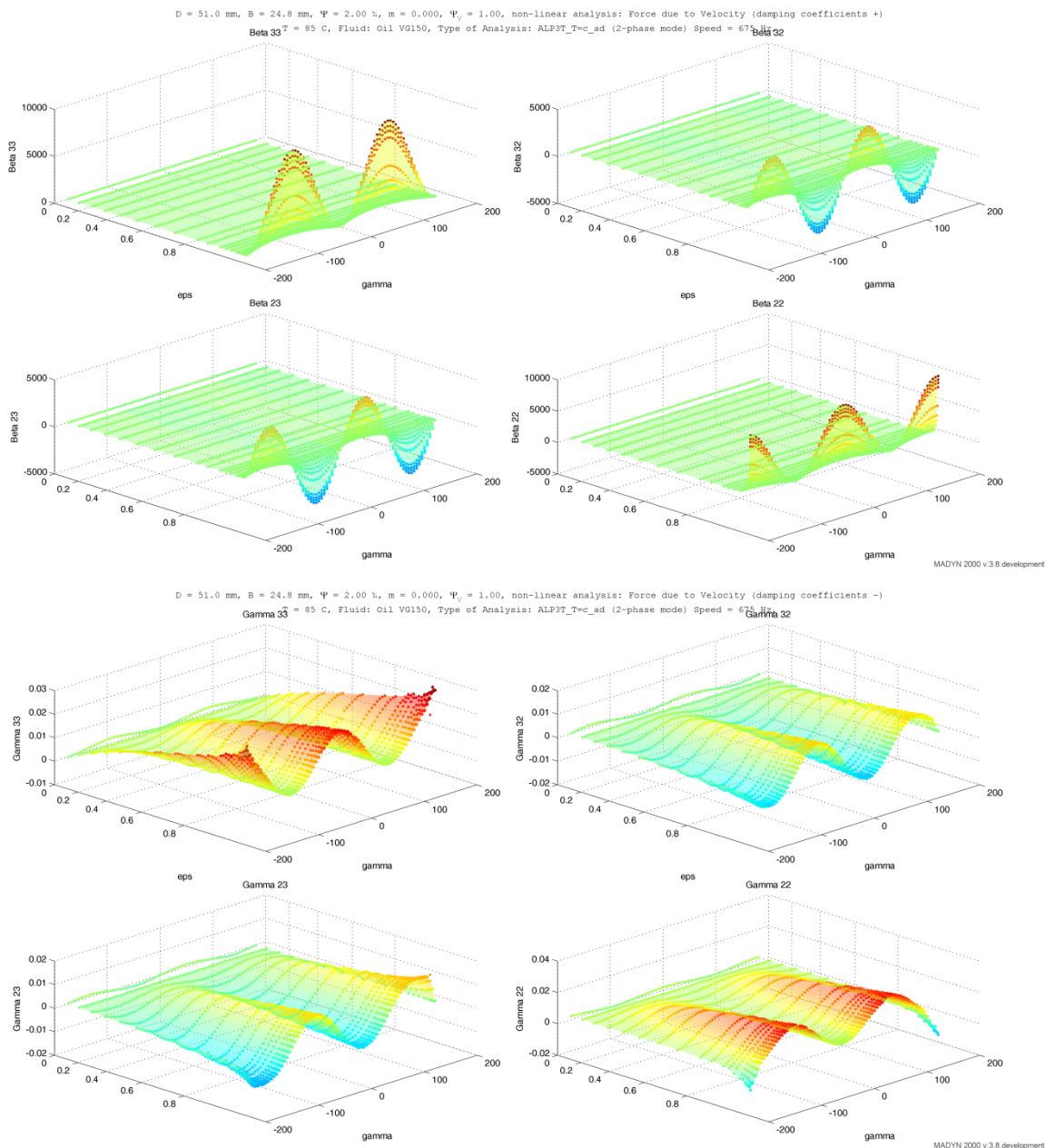


Fig. 8.3: Dimensionless damping coefficients β^+ (Beta) and β^- (Gamma) as a function of the journal position ϵ and γ



8.2 General Squeeze Film Damper (Standard Bearing)

A general squeeze film damper currently can be created as bearing type “Standard” and imported dimensionless data. The dimensionless table may stem from the inner film of a squeeze film damper. This is a temporary workaround, until a standalone squeeze film damper will be available.

9. Improvements and New Features for Fluid Film Bearings

9.1 General Improvements

The speed and convergence of ALP3T bearing analyses have been considerably improved. This helps for extreme cases such as tilting pad bearing with small preload and central support.

The hydrostatic pocket width can be defined. In previous releases it had a standard width of 98% bearing width. This feature is implemented since version 3.7.4 and described in the current documentation II.6.11

9.2 Closed Cylindrical Bearing

The RFB GUI for the closed bearing is shown in figure 9.1. To model this type of bearing the pad type “Closed” is introduced. In order to supply fresh lubricant to the bearing an axial pressure has to be defined for the closed bearing. Closed bearings do not have any pockets. The pad GUI therefore is simplified. It is shown in figure 9.2.

The analysis types of a closed bearing are restricted to ALP3T_T=c_ad (constant adiabatic) and ALP3T_T=v_ad (variable adiabatic) with 2-phase flow. This is due to the fact, that closed bearings mostly run in high ambient pressure and that cavitation in large areas is suppressed, which requires 2-phase flow for correct modelling.

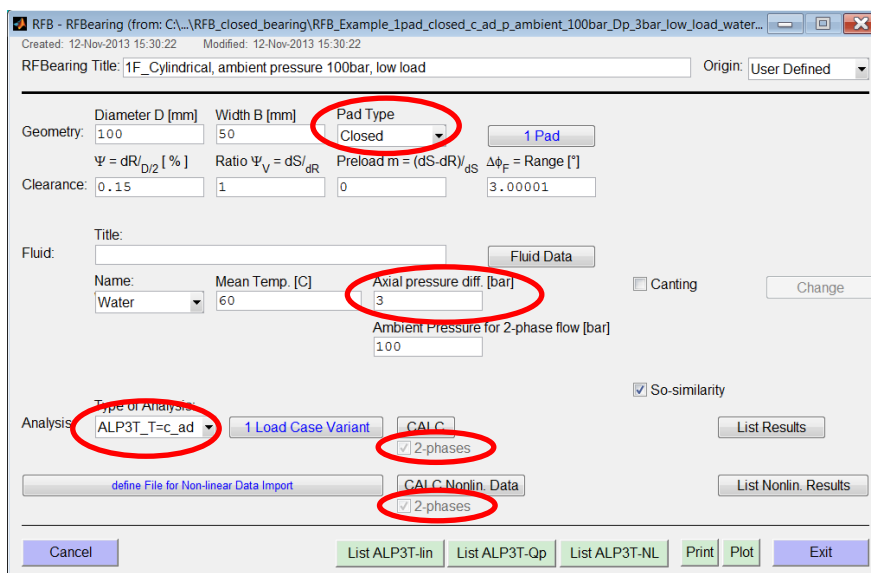


Fig. 9.1: RFB GUI for the closed bearing

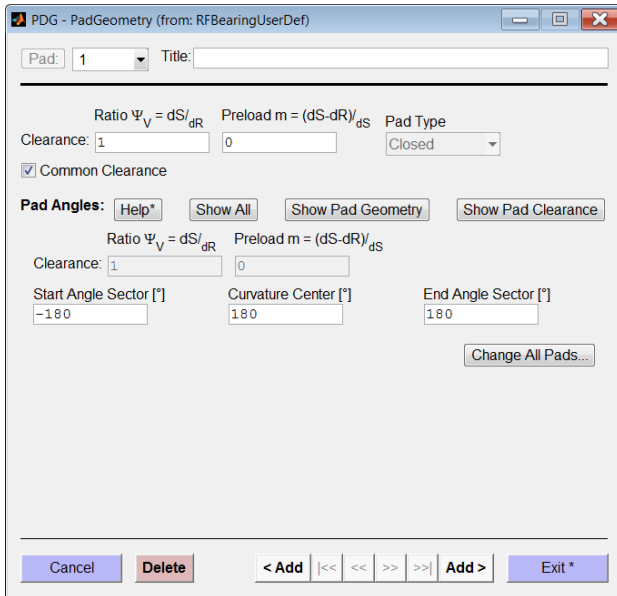


Fig. 9.2: Pad GUI for the closed bearing

The static results and coefficients of a cylindrical water lubricated bearing in high ambient pressure for a rather low load of 100N can be seen in figure 9.3 and 9.4. It can be clearly seen, that the position angle is 90° even at relatively low speed, that the stiffness matrix at elevated speed (> 50cps) is skew symmetric ($k_{32} = -k_{23}$, $k_{22} = k_{33} \approx 0$) and that the damping matrix is diagonal ($d_{23} = d_{32} \approx 0$) and equal in both directions $d_{22} = d_{33}$). These are typical characteristics for a low loaded closed cylindrical bearing.

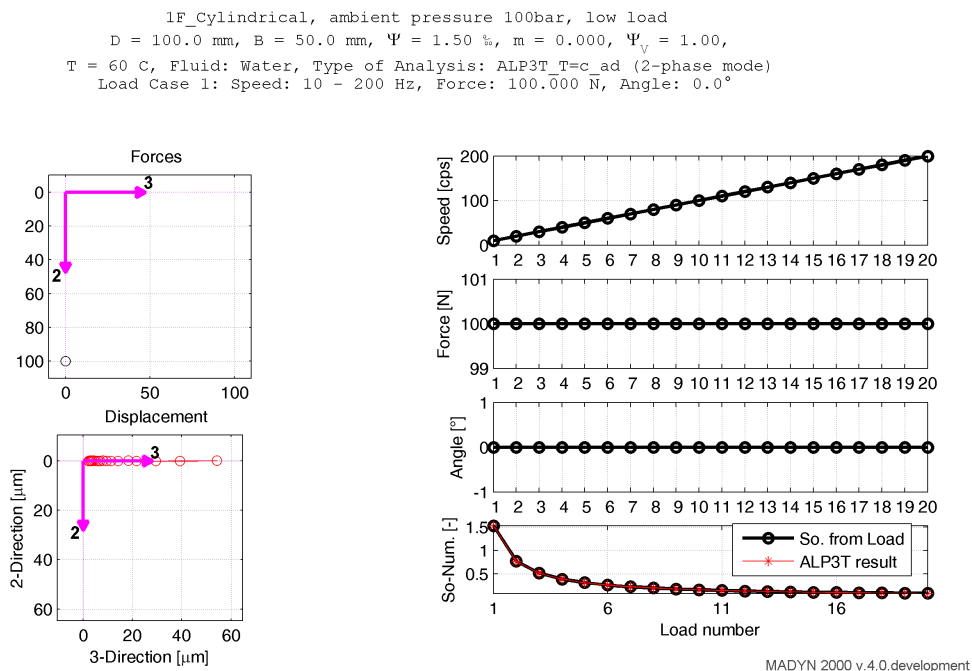


Fig. 9.3: Static results of a closed water lubricated bearing in high ambient pressure (100bar)

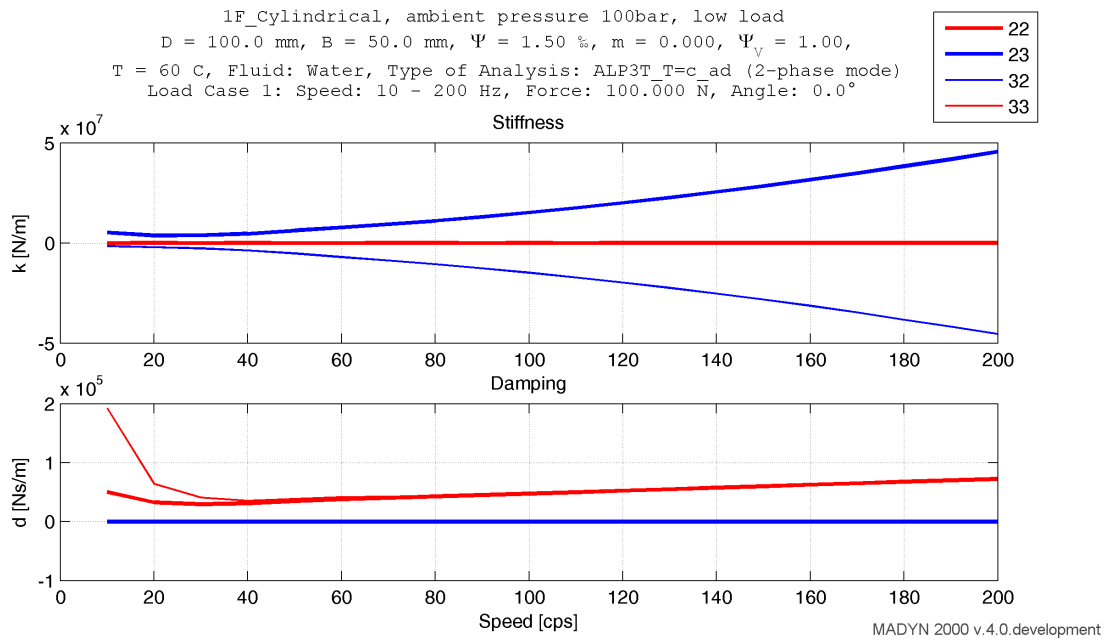


Fig. 9.3: Coefficients of a closed water lubricated bearing in high ambient pressure (100bar)



10. New Features for Static Analyses

10.1 Alignment Sensitivity Analysis

The alignment sensitivity analysis calculates the sensitivity of the bearing pressures (bearing forces per projected bearing area) and the shaft stresses at stations in case of a bearing lift of 1mm of each bearing relative to a base case. Typically the base case is a static load case with a weight and an alignment load, which represents an ideal alignment. The GUI to define an alignment sensitivity analysis is shown in figure 10.1. In the GUI the base case must be defined and stations for the stresses can be selected in "Result Selection". Bearing loads are always calculated and cannot be selected. Further analysis parameters are according to the base case.

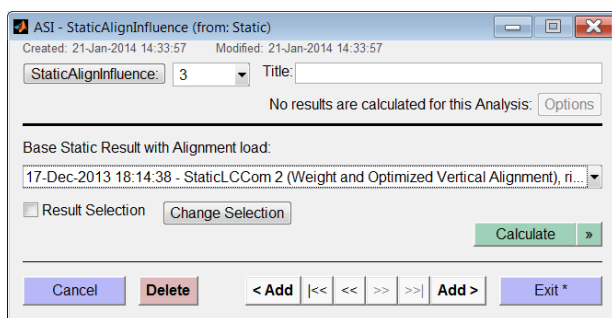
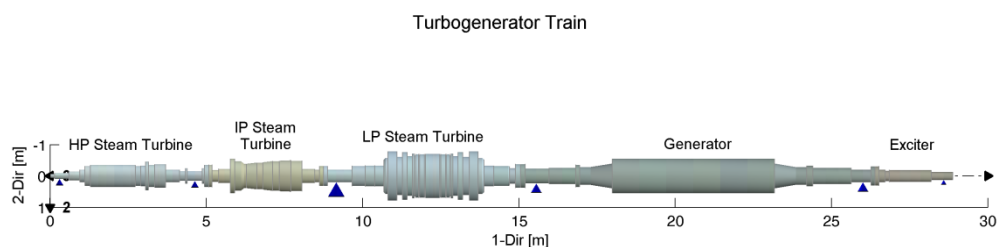


Fig. 10.1: GUI to define an alignment sensitivity analysis

It should be noted, that the shaft stresses for the alignment sensitivity are evaluated at stations, not in sections. Each station has two adjoining section, with potentially different stresses. The sensitivity is calculated for the higher of the two stresses in the base load case.

The results of a sensitivity analysis for the example in figure 10.2 are shown in the following. The rotor has six bearings, i.e. the sensitivity is calculated for six bearing lifts. The base load case and result are shown in figures 10.3 and 10.4.



MADYN 2000 v.4.0.development

Fig. 10.2: Example for the alignment sensitivity analysis

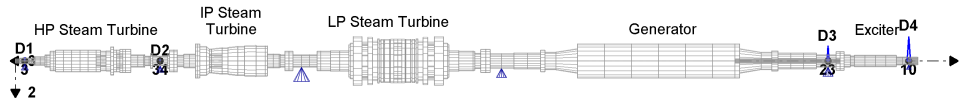


Turbogenerator Train

Static Loads

Load case: StaticLCCom 2 (Weight and Optimized Vertical Alignment)
 Gravitation:

$$g_1 = 0.00 \text{ m/s}^2, g_2 = 9.81 \text{ m/s}^2, g_3 = 0.00 \text{ m/s}^2$$



Label	Displacement 2-dir	Displacement 3-dir
D1	-1700 μm	0 μm
D2	-910.95 μm	0 μm
D3	-7400 μm	0 μm
D4	-11800 μm	0 μm

MADYN 2000 v.4.0.development

Fig. 10.3: Base load case

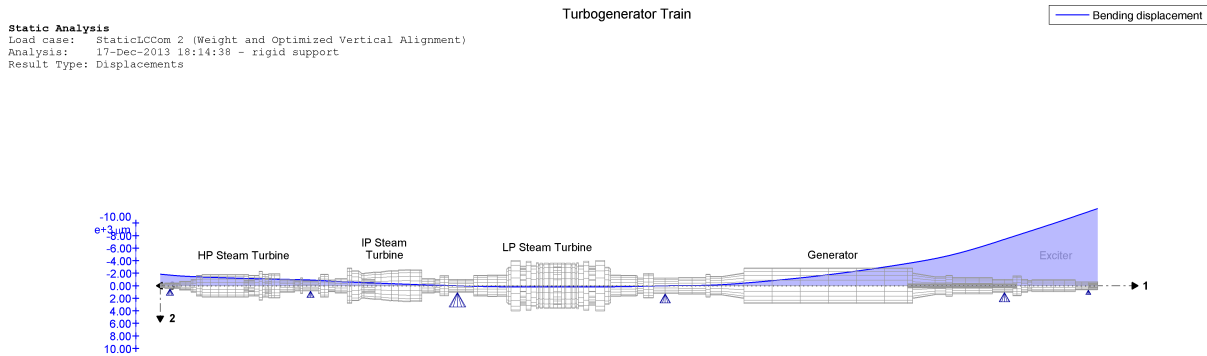


Fig. 10.4: Base load displacement result

The alignment sensitivity has only print, no plot outputs. The print can be seen in the following. The results of the base load and the sensitivities of the specific bearing loads and bending stresses at selected locations can be seen for the different bearing lifts B01 to B06. For the bearing forces as well as for the bending stresses the components in two directions are considered. The sensitivities are calculated from the magnitudes.

Static Analysis:
 with selection
 Created: 16-Dec-2013 18:04:40
 Modified: 16-Dec-2013 18:08:08

System:
 Turbogenerator Train
 TLA case: [1 0 0 1 0 0]

Analysis Parameters:

The analysis has been carried out with rigid bearings characteristic.



Result:

Created: 21-Jan-2014 10:58:15

Parameters of the result:

Relative Speed: 100.0%

Alignment Sensitivity Analysis

Base [MPa] - Reference Bearing Load or Shaft Stress
B01 [MPa/mm] - Shaft 1 (HP Steam Turbine): Station 3 (Bearing 1)
B02 [MPa/mm] - Shaft 1 (HP Steam Turbine): Station 34 (Bearing 2)
B03 [MPa/mm] - Shaft 3 (LP Steam Turbine): Station 3 (Bearing 3)
B04 [MPa/mm] - Shaft 4 (Generator): Station 3 (Bearing 4)
B05 [MPa/mm] - Shaft 4 (Generator): Station 23 (Bearing 5)
B06 [MPa/mm] - Shaft 5 (Exciter): Station 10 (Bearing 6)

RFB Specific Load

Station	Base	B01	B02	B03	B04	B05	B06
S1-03	1.3368	0.1907	-0.4048	0.2385	-0.0256	0.0016	-0.0003
S1-34	1.5099	-0.1310	0.4020	-0.3827	0.1174	-0.0072	0.0015
S3-03	1.8409	0.0443	-0.2198	0.3212	-0.1794	0.0424	-0.0086
S4-03	3.2621	-0.0048	0.0674	-0.1794	0.1726	-0.0947	0.0388
S4-23	1.8451	0.0003	-0.0045	0.0465	-0.1039	0.2128	-0.1512
S5-10	0.3264	-0.0003	0.0047	-0.0484	0.2178	0.1214	0.6006

Station Stresses

Station	Base	B01	B02	B03	B04	B05	B06
S1-04	8.6476	1.2690	-2.6944	1.5872	-0.1701	0.0104	-0.0021
S1-34	10.1949	-7.0222	14.9104	-8.7835	0.9411	-0.0576	0.0117
S1-35	4.6582	-2.7295	13.2082	-2.4517	0.2557	-0.0156	0.0032
S2-04	3.3599	1.8197	-2.8118	0.4172	0.6044	-0.0370	0.0075
S2-17	4.8426	0.2660	3.2624	-3.2529	3.0504	-0.1866	0.0380
S3-03	4.6156	0.5955	-0.7756	13.4491	-3.3524	0.3595	-0.0732
S3-37	7.4555	-0.0264	0.3748	0.4286	-1.4343	0.8252	-0.1680
S4-07	15.4612	0.0177	-0.2506	2.5740	-3.6899	1.3844	-0.0356
S4-17	25.3802	0.0028	-0.0398	0.4085	-0.1598	-1.9283	1.7165

10.2 Speed Dependent Loads

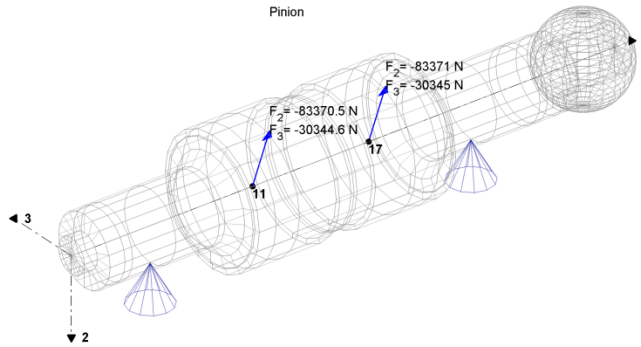
In version 4.0 speed dependent loads for static analyses can be defined. This feature is useful for example for gear shafts, which have a speed dependent mesh force. An example for such a load is shown in figure 10.5.

The GUI to define this speed dependent load is shown in figure 10.6. The speed dependence is defined by one or several functions, which are created in the function GUI shown in figure 10.7. The GUI is called by the highlighted button in figure 10.6. Defined functions can be assigned to forces in the load GUI by the drop down menu next to the edit field to define force values (marked in red). The forces are multiplied by the function values.

The further procedure to carry out a static analysis with speed dependent load is similar to any static analysis in a speed dependent system. Analyses with rigid supports, which are normally speed independent, become speed dependent.



Static Loads
 System from Pinion
 Load case: StaticLC 1 (Mesh Force, f(n) til 100%), speed-dependent



MADYN 2000 v.4.0.development

Fig. 10.5: Pinion with speed dependent mesh force

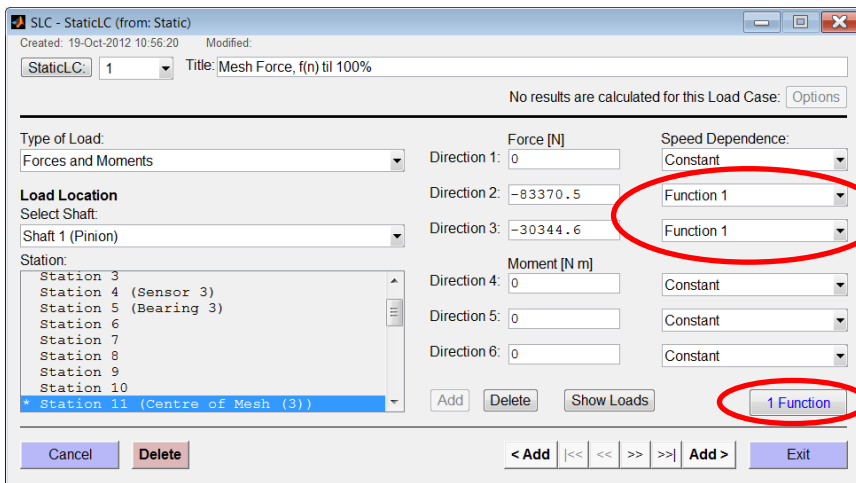
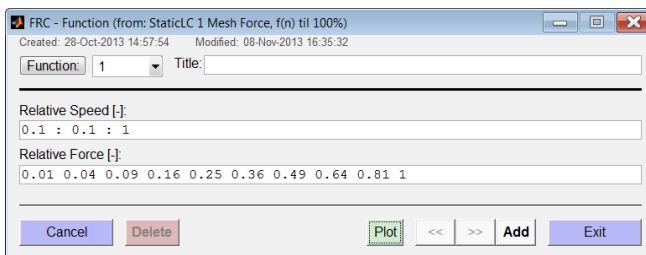
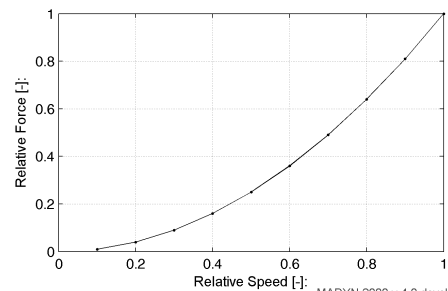


Fig. 10.6: Load GUI to define a speed dependent load



SLC - Relative Force as a Function of a Relative Speed



MADYN 2000 v.4.0.development

Fig. 10.7: Function GUI to define speed dependence with corresponding plot



11. Extension of Modelling Objects

11.1 General Spring (with off diagonal elements)

Until the last version the general spring GSP could only contain diagonal stiffness and damping values. In version 4.0 a full 6x6 matrix including off-diagonal elements can be defined as general spring.

The GSP GUI is shown in figure 11.1. As in previous versions it contains edit fields for the diagonal elements. Additionally it contains the highlighted buttons, which opens the GUI in figure 11.2 to define a full stiffness and/or damping matrix. The matrix can be saved to a text file and loaded from a text file. In case of loading the file must contain 6 rows and columns.

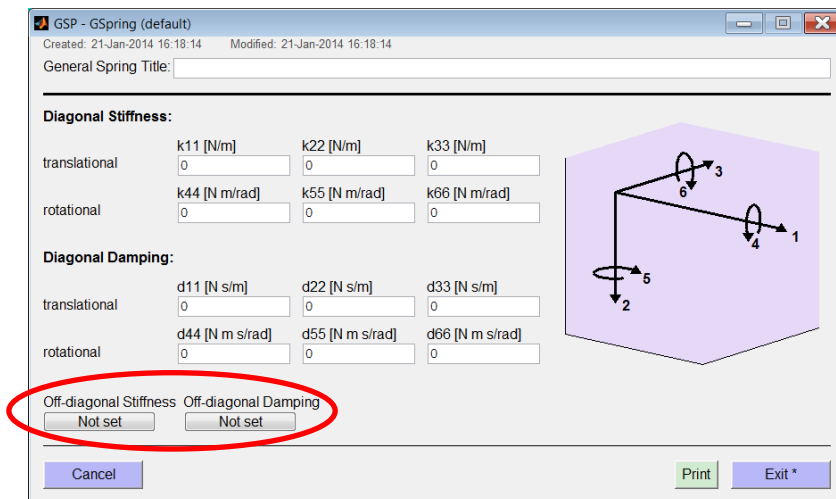


Fig. 11.1: GUI for the general spring GSP

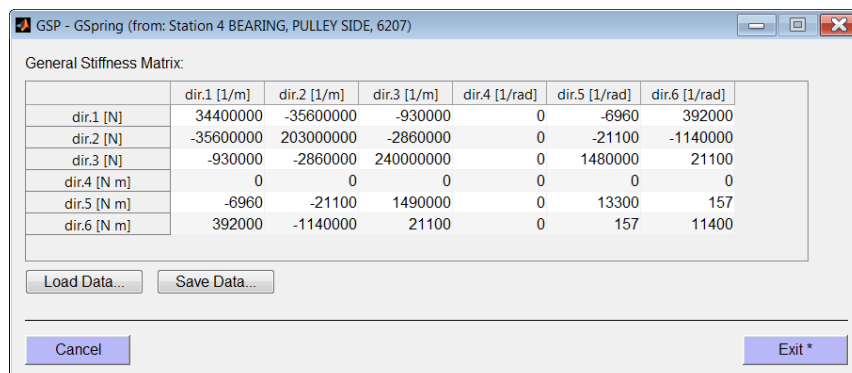


Fig. 11.2: GUI to define the full GSP matrix

It should be noted, that the full GSP matrix can be varied in stiffness and damping variation. This allows for example simulating a cross coupling stiffness variation for lateral stability analyses as it is required in API. A corresponding full GSP matrix is shown in figure 11.3. The result of the variation for the example in figure 11.4 for the 1st forward whirling bending can be seen in figure 11.5.

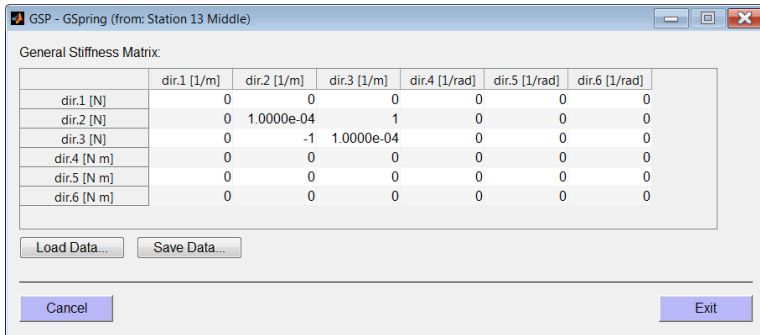
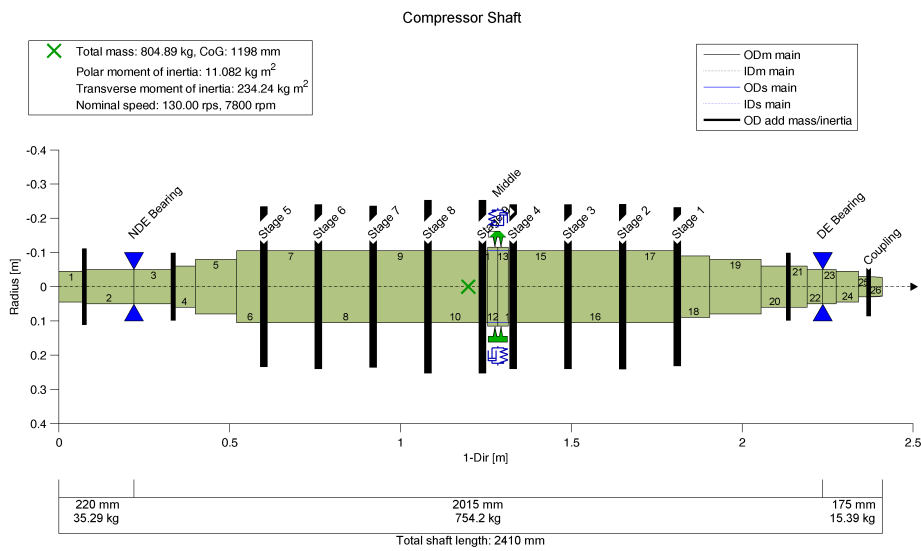


Fig. 11.3: GSP full matrix for lateral cross coupling variation to assess the rotor stability



MADYN 2000 v.4.0 development

Fig.11.4: Example rotor for cross coupling variation

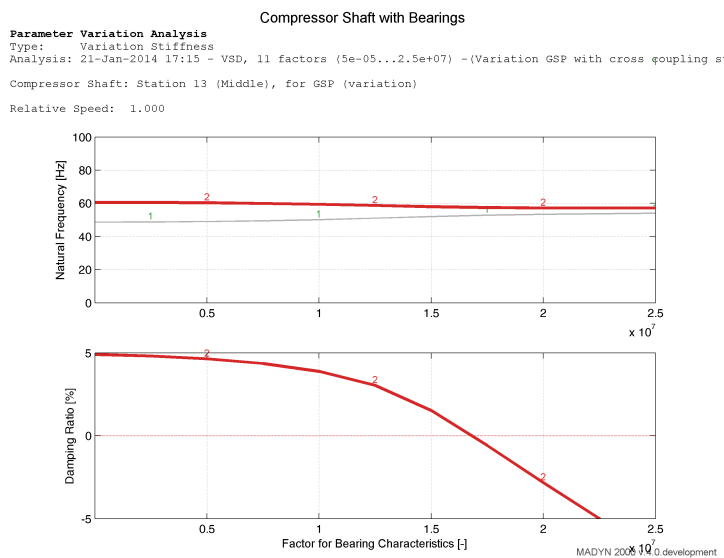


Fig. 11.5: Result of cross coupling variation to assess the rotor stability (also see API 617)



11.2 Flexible Coupling Damping

The GUI for the modelling of a flexible coupling in version 4.0 is shown in figure 11.6. The new edit field to define a damping coefficient for the coupling is highlighted. The dimensioned damping coefficient is directly used in the eigenvalue analysis and thus influences eigenvalues and mode shapes, whereas the “Damping Ratio” or “Dynamic Magnifier” calculates the effect of the coupling damping ratio on the damping ratio of a natural mode by multiplying the coupling damping ratio with the ratio of the deformation energy in the coupling to the deformation energy of the complete rotor. The shapes are not influenced by this value.

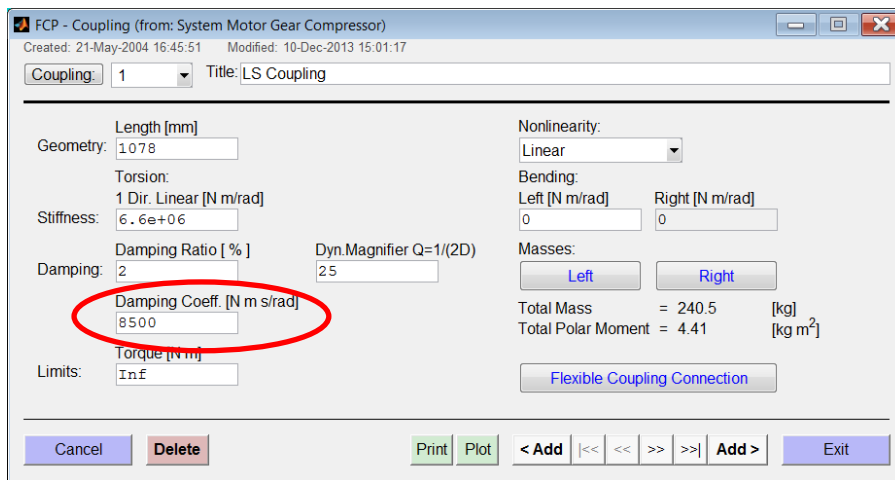


Fig. 11.6: Flexible coupling GUI with edit field for a damping coefficient

12. Improved Loading of Fluids

Fluid data of several fluids, which are in form of a table in text files can now be directly loaded to shafts. Until now the loading of such fluids to a shaft required several steps invoked from the menu item “Input FDC from File” of the menu “Extras”. The new shaft GUI with the highlighted button to load fluids is shown in figure 12.1. For the content of the text file the same rules apply as in previous versions.

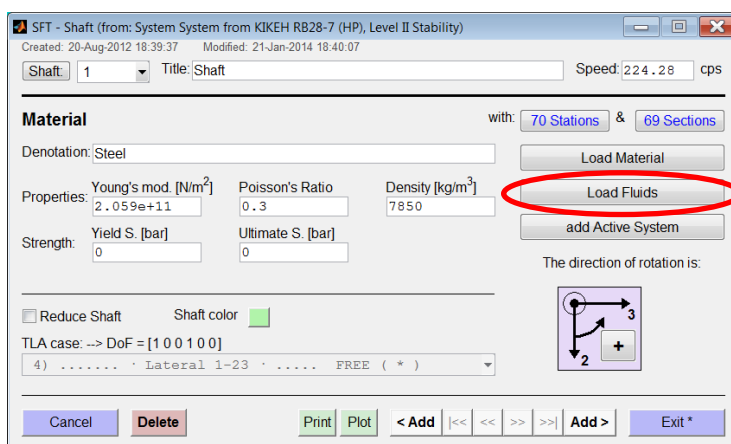


Fig. 12.1: Shaft GUI with button to load fluids



13. Improvements in Plots

13.1 Plot Editing

Plots can be edited, i.e. labels, legends ... by activating a button in the menu of each plot. The menu is shown in figure 13.1. The button for editing is highlighted in the figure.

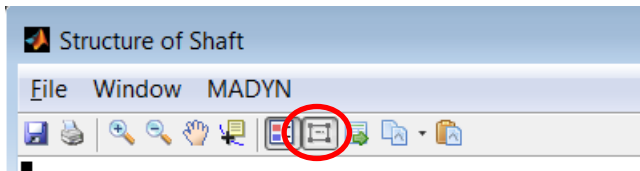


Fig. 13.1: Menu item for plot editing

13.2 Model Plots

In figure 13.2 a shaft plot is shown. The plot has the following new features:

- Station labels appear on the plot,
- solid sections are filled with a colour.

Controls for the appearance of the plot are shown in figure 13.3. The items “Fill Solid Sections” and “Show Station Labels” are new. The colour to fill the solid sections can be defined in the shaft GUI, by clicking on the corresponding symbol (see figure 13.4).

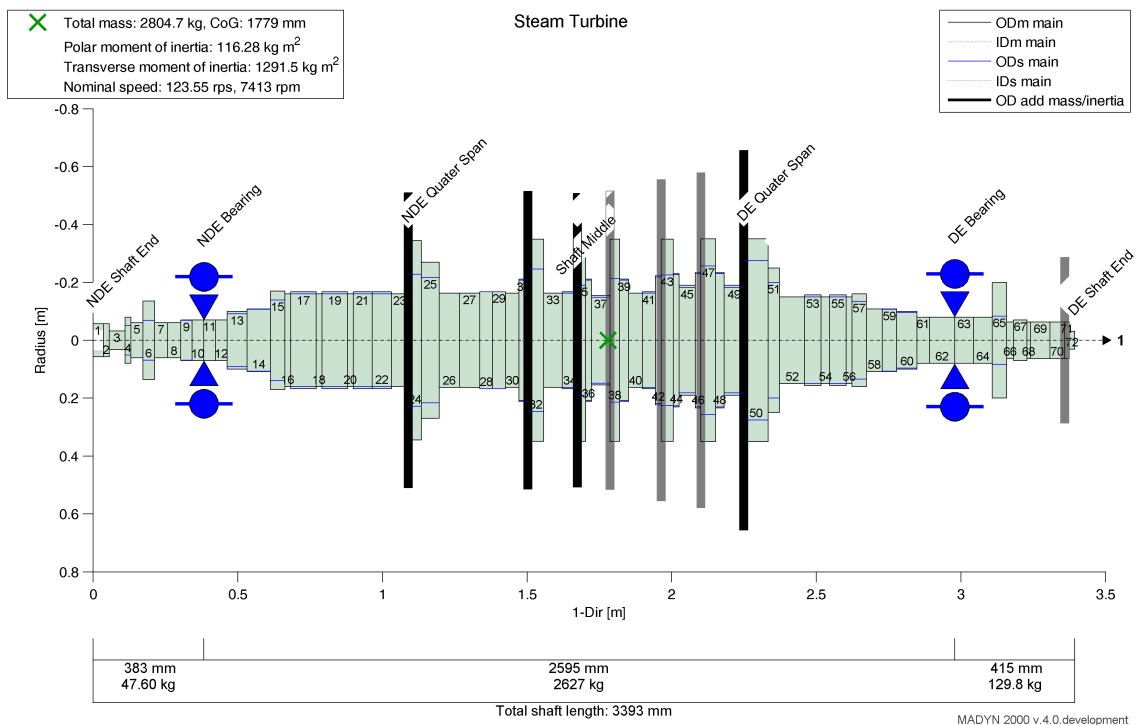


Fig. 13.2: Shaft plot

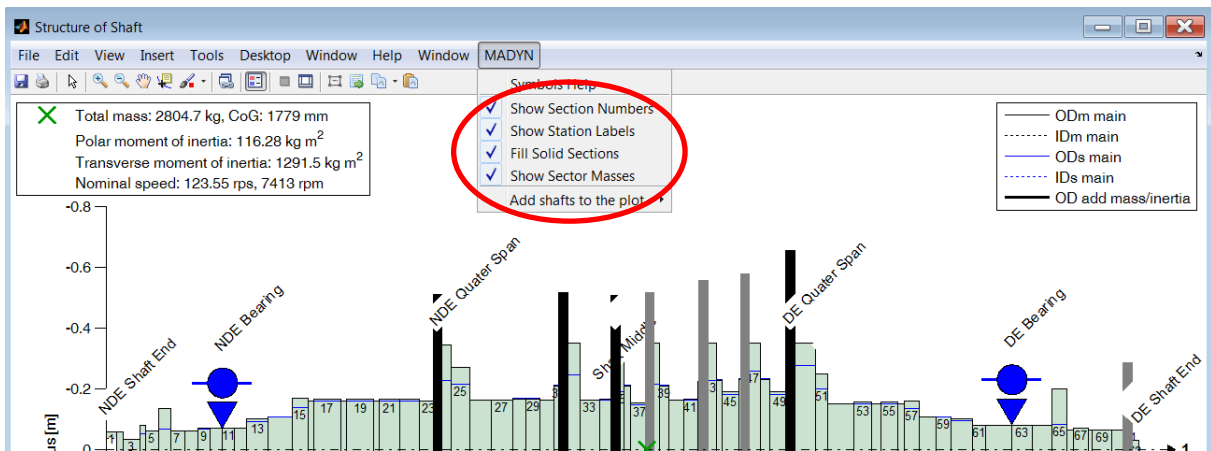


Fig. 13.3: Shaft plot controls in the MADYM menu

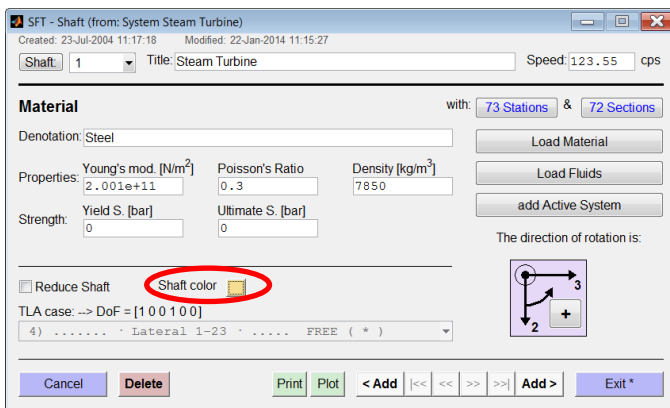


Fig. 13.4: Shaft GUI with controls to select the colour of the shaft plot.

Shaft plots are now possible for several shafts, i.e. shafts of a system can be added to the plot. The shaft plot can also be called from the system plot as shown in figure 13.5. The corresponding plot is shown in figure 13.6. In case the system has shafts with different axes, the summary of data (inertias and speeds) is shown for each axis separately. Shafts can be added or eliminated from the plot by the controls shown in figure 13.7.

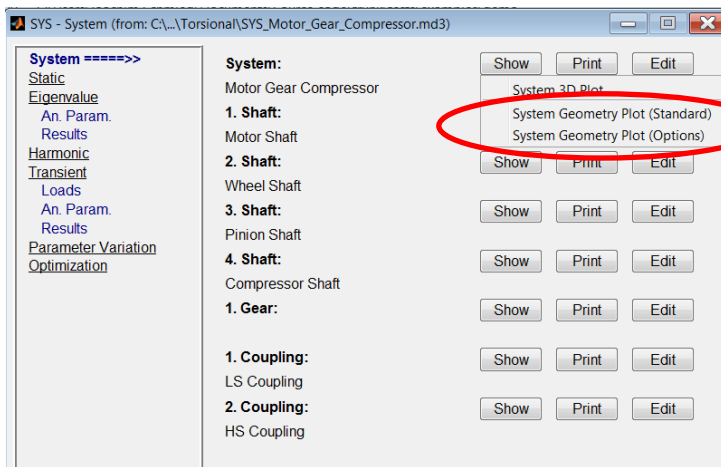


Fig. 13.5: Controls to call a shaft plot of the system

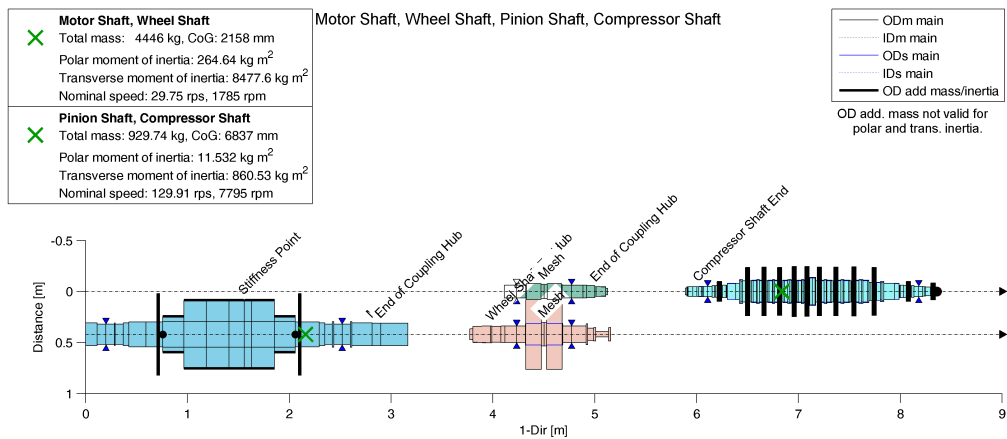


Fig. 13.6: Plot of a system with all shafts

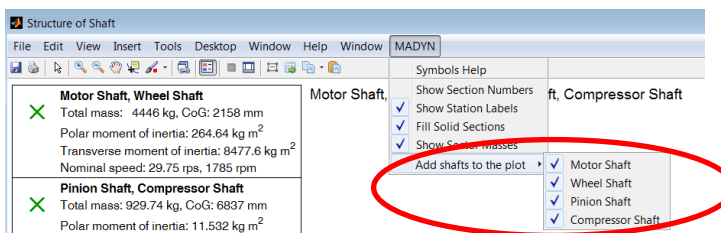


Fig. 13.7: Controls to add or eliminate shafts



13.2 Shape Plots (data cursor)

Data cursors can now be added to shape plots in a similar way as to diagram plots. An example is shown in figure 13.8. Moreover the data cursor now contains information about the meaning of the values.

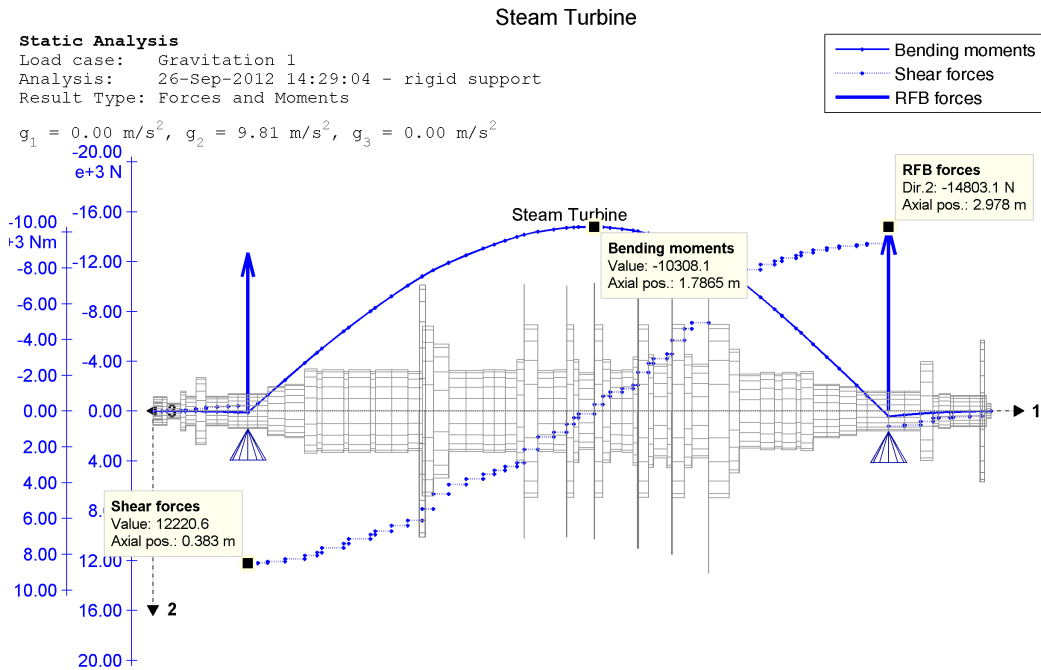


Fig. 13.8: Shape plot of shaft forces with added data cursors



14. Improvements in Prints

14.1 System Print

The system print now contains the following auxiliary data of each shaft as shown below for the system in figure 13.5:

Length
Centre of Gravity (CoG)
Mass
Weight
Polar moment of inertia
Torsional stiffnesses from end to end, left end to CoG, CoG to right end

System:

Motor Gear Compressor
Created: 23-Jul-2004 11:29:39
Modified: 22-Jan-2014 11:44:17
Length = 8373.78 mm
Mass = 5661.48 kg
Weight = 55520.19 N

The system consists of the following components:

4 Shafts

1.Motor Shaft
Created: 23-Jul-2004 11:28:40
Modified: 22-Jan-2014 11:44:15
n = +1785.00 rpm
Length = 3164 mm
CoG = 1456.7 mm
Mass = 3415.4 kg
Weight = 33493 N
Polar Moment of Inertia = 212.96 kg m²
Torsional Stiffness:
end to end = 7155.1 kN m/rad
left end to CoG = 16148 kN m/rad
CoG to right end = 12848 kN m/rad

2.Wheel Shaft
Created: 23-Jul-2004 11:29:16
Modified: 22-Jan-2014 11:44:17
n = +1785.00 rpm
Length = 1384.2 mm
CoG = 710.19 mm
Mass = 1030.7 kg
Weight = 10107 N
Polar Moment of Inertia = 51.677 kg m²
Torsional Stiffness:
end to end = 479.08 kN m/rad
left end to CoG = 7187.3 kN m/rad
CoG to right end = 513.29 kN m/rad

3.Pinion Shaft
Created: 23-Jul-2004 11:29:23
Modified: 22-Jan-2014 11:44:17
n = -7794.61 rpm
Length = 1014.3 mm
CoG = 462.63 mm
Mass = 108.63 kg
Weight = 1065.3 N
Polar Moment of Inertia = 0.25736 kg m²
Torsional Stiffness:
end to end = 1512.4 kN m/rad
left end to CoG = 5943.3 kN m/rad
CoG to right end = 2028.6 kN m/rad

4.Compressor Shaft
Created: 23-Jul-2004 11:28:53
Modified: 22-Jan-2014 11:44:16
n = -7794.61 rpm
Length = 2485.1 mm
CoG = 1248 mm
Mass = 821.11 kg
Weight = 8052.4 N
Polar Moment of Inertia = 11.274 kg m²
Torsional Stiffness:
end to end = 486.05 kN m/rad
left end to CoG = 1570.2 kN m/rad
CoG to right end = 703.96 kN m/rad



14.2 Print of Radial Fluid Film Bearings

Since version 3.6 the thermo-elastic deformation of pads in tilting pad bearings can be considered in RFB analysis type "ALP3T_T=v_ad". These deformations now appear separately in the print as shown below for the bearing in figure 14.1. The thermal and elastic deformation for each pad are shown for each load case.

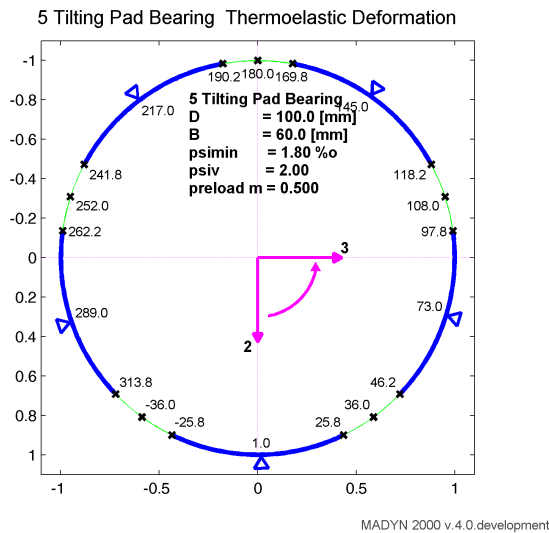


Fig. 14.1: Example bearing for the print of the thermo-elastic deformation

Thermal Deformations

speed [rpm]	F [N]	Angle [o]	d(dR) [um]	
Pad d(psiv)				
1 6.000e+02	4.000e+03	0.000e+00	-2.990e-01	
1 5.000e-03	2 5.000e-03	3 2.000e-03	4 1.000e-03	5 1.000e-03
2 1.200e+03	4.000e+03	0.000e+00	-7.721e-01	
1 1.295e-02	2 8.976e-03	3 2.994e-03	4 1.000e-03	5 1.994e-03
3 1.800e+03	4.000e+03	0.000e+00	-1.326e+00	
1 2.092e-02	2 1.395e-02	3 4.981e-03	4 1.000e-03	5 2.990e-03
4 2.400e+03	4.000e+03	0.000e+00	-1.903e+00	
1 2.690e-02	2 1.794e-02	3 7.951e-03	4 2.968e-03	5 3.984e-03
5 3.000e+03	4.000e+03	0.000e+00	-2.521e+00	
1 4.163e-02	2 1.995e-02	3 7.025e-03	4 1.049e-03	5 4.000e-03
6 3.600e+03	4.000e+03	0.000e+00	-3.220e+00	
1 3.811e-02	2 2.583e-02	3 1.381e-02	4 4.889e-03	5 4.972e-03
7 4.200e+03	4.000e+03	0.000e+00	-3.861e+00	
1 5.242e-02	2 2.888e-02	3 1.304e-02	4 2.115e-03	5 5.000e-03
8 4.800e+03	4.000e+03	0.000e+00	-4.588e+00	



- 52 -

```
1 5.012e-02 2 3.380e-02 3 1.877e-02 4 6.805e-03 5 5.961e-03

9      5.400e+03   4.000e+03   0.000e+00   -5.228e+00
1 6.609e-02 2 3.684e-02 3 1.711e-02 4 3.214e-03 5 6.000e-03

10     6.000e+03   4.000e+03   0.000e+00   -5.952e+00
1 7.367e-02 2 3.986e-02 3 1.795e-02 4 3.000e-03 5 6.000e-03

11     6.600e+03   4.000e+03   0.000e+00   -6.507e+00
1 8.720e-02 2 4.094e-02 3 1.706e-02 4 1.714e-04 5 6.000e-03

12     7.200e+03   4.000e+03   0.000e+00   -7.208e+00
1 8.610e-02 2 4.669e-02 3 2.174e-02 4 2.845e-03 5 6.000e-03
```

Elastic Deformations

```
speed [rpm] F [N] Angle [o] d(dR) [um]
Pad d(psiv) Pad d(psiv) Pad d(psiv) Pad d(psiv) Pad d(psiv)
1      6.000e+02   4.000e+03   0.000e+00   0.000e+00
1 1.300e-02 2 1.000e-03 3 0.000e+00 4 0.000e+00 5 1.000e-03

2      1.200e+03   4.000e+03   0.000e+00   0.000e+00
1 1.300e-02 2 1.000e-03 3 0.000e+00 4 0.000e+00 5 1.994e-03

3      1.800e+03   4.000e+03   0.000e+00   0.000e+00
1 1.300e-02 2 1.990e-03 3 0.000e+00 4 0.000e+00 5 2.000e-03

4      2.400e+03   4.000e+03   0.000e+00   0.000e+00
1 1.300e-02 2 2.000e-03 3 9.838e-04 4 9.838e-04 5 2.984e-03

5      3.000e+03   4.000e+03   0.000e+00   0.000e+00
1 1.300e-02 2 2.975e-03 3 1.000e-03 4 1.000e-03 5 3.000e-03

6      3.600e+03   4.000e+03   0.000e+00   0.000e+00
1 1.300e-02 2 3.000e-03 3 1.000e-03 4 1.000e-03 5 3.000e-03

7      4.200e+03   4.000e+03   0.000e+00   0.000e+00
1 1.300e-02 2 3.000e-03 3 1.000e-03 4 1.000e-03 5 3.000e-03

8      4.800e+03   4.000e+03   0.000e+00   0.000e+00
1 1.300e-02 2 3.000e-03 3 1.000e-03 4 1.000e-03 5 3.961e-03

9      5.400e+03   4.000e+03   0.000e+00   0.000e+00
1 1.300e-02 2 3.947e-03 3 1.000e-03 4 1.000e-03 5 4.000e-03

10     6.000e+03   4.000e+03   0.000e+00   0.000e+00
1 1.300e-02 2 4.000e-03 3 1.000e-03 4 1.000e-03 5 4.000e-03

11     6.600e+03   4.000e+03   0.000e+00   0.000e+00
1 1.300e-02 2 4.000e-03 3 1.000e-03 4 1.000e-03 5 4.000e-03

12     7.200e+03   4.000e+03   0.000e+00   0.000e+00
1 1.300e-02 2 4.000e-03 3 1.948e-03 4 1.000e-03 5 4.000e-03
```



- 53 -

References

/1/ Documentation of the MESYS rolling bearing analysis software.